UNIVERSITA' DEGLI STUDI DI VERONA

DEPARTMENT OF MEDICINE

GRADUATE SCHOOL FOR HEALTH AND LIFE SCIENCE

DOCTORAL PROGRAM IN

IMMUNITY, INFLAMMATION AND CANCER

Cycle/year XXXVI / 2020

TITLE OF THE DOCTORAL THESIS

Exploring the Complex Interplay between Myeloid-Derived Suppressor Cells (MDSCs), Interleukins, and Immune Checkpoint Inhibitors (ICIs) in Non-Small Cell Lung Cancer (NSCLC)

S.S.D. MED/06

Coordinator: Prof.
VINCENZO CORBO

Signature _____

Tutor: Prof.
MICHELE MILELLA

Signature _____

Doctoral Student: Dott.
LORENZO BELLUOMINI

Signature _____

Exploring the Complex Interplay between Myeloid-Derived Suppressor Cells (MDSCs), Interleukins, and Immune Checkpoint Inhibitors (ICIs) in Non-Small Cell Lung Cancer (NSCLC) – Lorenzo Belluomini

Ph.D. Thesis

Verona, 7 dicembre 2023

SOMMARIO

In considerazione del ruolo centrale del trattamento immunoterapico, associato o meno ad un trattamento chemioterapico, nel contesto del tumore del polmone non a piccole cellule (NSCLC), risulta cruciale una valutazione comprensiva dell'interazione tra la terapia con inibitori del checkpoint immunitario (ICI) e il *milieu* immunologico circolante.

La prima parte prospettica di questa tesi si propone di esaminare l'impatto della terapia con ICI sulle *myeloid-derived suppressor cells* (MDSCs) e più in generale sul microambiente immunologico circolante. Questa analisi ha coinvolto trentaquattro pazienti affetti da NSCLC avanzato, rivelando una riduzione significativa di citochine pro-infiammatorie, tra cui Interleuchina-8 (IL-8), esclusivamente nei pazienti *non-progressors* (NP) dopo il trattamento con ICI. Specificatamente, è stata dimostrata una significativa diminuzione dell'espressione di c-FLIP nelle MDSC monocitiche (M-MDSC) dei pazienti NP, suggerendo un possibile ruolo della terapia con ICI nel mitigare l'infiammazione sistemica e nell'inibire l'immunosoppressione dipendente dalle MDSC.

Nell'ottica di una valutazione/validazione del ruolo prognostico di IL-8 nel tumore del polmone, è stata quindi eseguita una metanalisi che includeva studi su pazienti sottoposti a differenti approcci terapeutici, quali immunoterapia, chemioterapia, chirurgia o inibitori della tirosin-chinasi. Tredici studi sono stati analizzati. Elevati livelli di IL-8 sono risultati associati ad una significativa riduzione della sopravvivenza complessiva (OS) nei pazienti affetti da tumore del polmone, in particolare quelli trattati con immunoterapia. Inoltre, attraverso un'analisi di OS utilizzando dati di RNA-seq provenienti dal *The Cancer Genome Atlas (TCGA)*, l'alta espressione di IL-8 nei pazienti con cancro polmonare è stata correlata ad una peggiore OS rispetto ai pazienti con bassa espressione di IL-8. Le analisi di sottogruppo hanno inoltre dimostrato una significativa differenza sia nella sopravvivenza libera da progressione (PFS) che nella OS tra i pazienti trattati con chemioterapia/ICI e altri trattamenti, inclusi terapie a target molecolare.

Integrando i risultati provenienti da entrambi gli studi, questa tesi offre una comprensione approfondita della complessa relazione tra la terapia con ICI e il microambiente immunologico circolante nel contesto del NSCLC. I risultati suggeriscono che la terapia con ICI può modulare la risposta immunitaria, riducendo l'infiammazione sistemica e compromettendo l'immunosoppressione dipendente dalle MDSC. Inoltre, la metanalisi sottolinea l'effetto prognostico negativo dei livelli elevati di IL-8, specialmente nei pazienti sottoposti a immunoterapia, evidenziando le potenziali implicazioni cliniche di questi risultati nella gestione del paziente affetto da tumore del polmone.

ABSTRACT

In the era of immunotherapy, exploring the interplay between immune checkpoint inhibitor (ICI) therapy and myeloid-derived suppressor cells (MDSCs), as well as Interleukins, in non-small cell lung cancer (NSCLC) appears intriguing. The first prospective part of this thesis investigates the impact of ICI therapy on the immunological landscape and the expression of cellular FLICE (FADD-like interleukin-1β-converting enzyme)-inhibitory protein (c-FLIP) in MDSCs. Thirty-four NSCLC patients were longitudinally analyzed, revealing a reduction in pro-inflammatory cytokines exclusively in non-progressors (NP) after ICI treatment. Through advanced analysis techniques, a distinctive decrease in c-FLIP expression in monocytic (M)-MDSCs from NP patients was identified, suggesting a potential role of ICI therapy in mitigating systemic inflammation and impairing MDSC-dependent immunosuppression.

The second study, a comprehensive meta-analysis, focuses on the prognostic role of IL-8 in lung cancer in patients undergoing different treatment approaches (immunotherapy, chemotherapy, surgery, or tyrosine kinase inhibitors). Thirteen studies encompassing different lung cancer stages were included in the analysis. High levels of IL-8 were associated with a significantly shorter overall survival (OS) in patients, particularly those treated with immunotherapy. Moreover, through OS analysis using RNA-seq data from The Cancer Genome Atlas (TCGA), the high expression of IL8 in patients with lung cancer was associated with worse OS than patients with low IL8 expression.

By merging the insights from these two analyses, this thesis provides a comprehensive understanding of the intricate relationship between ICI therapy, the immunological landscape, and the prognostic impact of IL-8 in NSCLC. The findings suggest that ICI therapy can modulate the immune response, reducing systemic inflammation and impairing MDSC-dependent immunosuppression. Moreover, the meta-analysis underscores the negative prognostic impact of high IL-8 levels, particularly in patients treated with immunotherapy, highlighting the potential clinical implications of these findings in the management of lung cancer.

SUMMARY

1. INTRODUCTION

1.1 Epidemiology of Lung Cancer in Italy

1.1.1 Incidence, Mortality, and Survival

In Italy, approximately 41,000 new cases of lung cancer were estimated in 2020, with 27,550 in men and 13,300 in women, making it the second most common cancer in men (14%) and the third in women (7%) [1]. Lung cancer is more prevalent in males, ranking second only to prostate cancer, with incidence rates of 14% in the 50-69 age group and 17% in those over 70. In females, it ranks third in the 70+ age group (8%) and fourth in the 50-69 age group (7%). In recent years, incidence has declined among men (-1.7%), particularly in the 50-69 age group (-6.2%). In comparison, it has increased among women (+3.4%), especially in the 70+ age group, primarily attributed to the increased prevalence of smoking in females since the late 1980s [1].

Lung cancer is the leading cause of cancer-related deaths in men and the second in women. In 2017, approximately 34,000 deaths were recorded in Italy, with 23,400 in men and 10,000 in women [1]. The 5-year survival rate for lung cancer patients in Italy is 15% in men and 19% in women, negatively influenced by numerous diagnoses at an advanced stage [1].

1.1.2 Prevalence and Cure

In 2020, there were estimated to be over 117,000 individuals in Italy living with a past diagnosis of lung cancer, including 77,200 men and 40,600 women [1]. The prevalence indicates that 34% of individuals have had a lung cancer diagnosis for less than two years, 23% for 2-5 years, 17% for 5-10 years, while only 25% received a diagnosis over ten years ago [1]. The estimated cure rate for lung cancer patients diagnosed in Italy in 2000 is 8% in men and 13% in women [1,2].

1.2 Risk Factors

Approximately 103,000 of the 127,070 lung cancer deaths (81%) in 2023 will be caused by cigarette smoking directly, with an additional 3560 caused by second-hand smoke [3]. Cigarette smoking accounts for 85%-90% of lung cancer cases, making it the most significant risk factor for cancer development [4]. The relative risk of developing lung cancer is directly associated with the number of cigarettes smoked per day, the duration of smoking habits, and the tar content of cigarettes [2]. The relative risk for smokers compared to non-smokers is 14, while that for heavy smokers, defined by smoking more than 20 cigarettes a day, is 20. Smoking cessation leads to a gradual reduction in risk over the next 10-15 years, with a significant advantage in gained years of life for those who quit before 40 [5]. Non-smokers exposed to passive smoke also have an increased risk of developing lung cancer, ranging from 20% to 50% compared to non-smokers [6,7].

Among other risk factors, various substances of occupational and environmental origin, such as asbestos, radon, chromium, arsenic, beryllium, vinyl chloride, polycyclic aromatic hydrocarbons, chloromethyl ether, and others, have been recognized as lung carcinogens by the International Agency for the Research on Cancer (IARC). In the presence of tobacco smoke, these substances have a synergistic effect that exponentially increases their carcinogenic activity [1]. The role of exposure to delicate particulate matter and air pollution is also recognized. The AHSMOG-2 study, assessing the association between fine particles (PM2.5) and lung cancer in non-smokers, found a 22% increase in the risk of neoplasm for every 10-µg/m3 increase in PM2.5 in the environment [8]. In the "ESCAPE" study, a 55% increase in the risk of developing lung adenocarcinomas, the most common histotype in non-smokers, was observed in [9]. Finally, a marginal role of genetic predisposition, particularly genetic polymorphisms, is demonstrated, although environmental exposure remains dominant in lung cancer etiology [10].

1.3 Histopathological Classification

Lung cancer is a heterogeneous group of diseases in both morphology and molecular subtypes. There are two main histological categories of lung cancer:

small-cell lung cancer (SCLC) (13% of cases) and non-small-cell lung cancer (NSCLC) (76% of cases). NSCLCs include a variety of histological forms, primarily adenocarcinoma, and squamous cell carcinoma.

1.3.1 Squamous Cell Carcinoma (CS)

Representing about 25% of all lung cancer cases, CS exhibits a strong correlation with cigarette smoking. Originating from proximal bronchi, CS has been often diagnosed as a central/hilar mass and tends to expand, invading the basement membrane and the luminal side of the bronchi, causing obstruction and atelectasis [11]. CS is characterized by slower growth than other histotypes, with an estimated three to four years needed to transition from in situ carcinoma to clinically evident tumor [11]. The neoplastic cells tend to spontaneous exfoliation, enabling early diagnosis through cytological examination of sputum. However, bronchoscopy with biopsy remains preferred diagnostic method[11].

1.3.2 Adenocarcinoma (ADC)

Comprising approximately 40% of all lung cancer cases, ADC's incidence is on the rise, especially in females. Originating from the surface epithelium or glands of the bronchial mucosa, it is more often located peripherally [11]. ADC demonstrates a more aggressive disease course compared to CS, with a tendency to rapidly metastasize through the bloodstream and invade the pleura [11].

1.3.3 Small Cell Carcinoma (SCLC)

Accounting for about 15% of all lung cancer cases, SCLC is strongly associated with smoking habits [11]. It usually originates centrally and is an aggressive histology with a high potential for distant dissemination. Consequently, metastases are frequently diagnosed before the primary tumor [11]. SCLC exhibits high proliferative kinetics, a short doubling time, and a high mitotic

index, with rapid disease progression and survival of approximately six weeks without treatment [11].

1.3.4 Large Cell Carcinoma (CGC)

Among the four prevalent histotypes, CGC represents the least common, accounting for approximately 10% of all lung cancer cases, often diagnosed through exclusion [11]. Its clinical behavior does not present distinctive features, and the prognosis is similar to that of adenocarcinoma [11].

1.4 Diagnostic and Staging Procedure

1.4.1 Clinical Presentation

The clinical presentation in most cases is nonspecific, and the onset of symptoms is often late. It is not uncommon for the diagnosis to be made when the disease is already in a metastatic phase, especially in cases of small-cell lung carcinoma [11]. The onset symptoms can be categorized as local, resulting from tumor growth; regional, resulting from the primary tumor extension and lymph node invasion; and systemic, due to secondary manifestations [11]. Paraneoplastic syndromes, which can occur even in the absence of other symptoms and metastases and without a pathogenetic correlation with the tumor, are among the ways the disease can manifest [11].

1.4.2 Diagnostic/Staging procedure following suspected cancer

A detailed medical history and thorough patient physical examination are essential for a precise diagnostic evaluation. Regarding the clinical history, it is crucial to investigate smoking habits. Other fundamental factors to assess include comorbidities, weight loss, anorexia, performance status, family history of neoplasms, and the patient's mental state [1,11]. The physical examination should be carefully performed on the entire body to guide the diagnosis and gather

information about the extent of the disease [11]. The subsequent diagnostic and clinical staging phase requires the rational use of modern imaging techniques and sampling [1]. Chest X-rays are crucial in locating and characterizing lung masses, raising suspicion of neoplasia [11]. Additionally, it can help identify hilar and mediastinal lymph node metastases, atelectatic areas, pleural effusion, and diaphragmatic elevation, a sign of phrenic nerve paralysis [11]. The following diagnostic investigation involves a CT scan of the chest, upper abdomen, and lower cervical region to examine other organs potentially involved in metastases, such as the liver, adrenal glands, and supraclavicular lymph nodes [12]. In current practice in Italy, in non-squamous histologies and cases where staging does not reveal a first-stage disease, brain CT is included from the beginning, even in clinically asymptomatic patients [12]. In cases where CT does not detect distant metastases, staging must be completed with 18F-FDG PET-CT (positron emission tomography with 18-fluorodeoxyglucose associated with CT). To consider the patient for surgical intervention, operability must be verified based on their health status, explicitly evaluating respiratory, cardiovascular, and metabolic function [12]. CT, in contrast, represents the main exam for staging, as it can provide adequate information on defining T, N, and M parameters, especially with integrating any additional tests [12]. MRI generally includes information similar to CT, except for the hilar region of the lung and the brain, where the data obtained is superior due to greater specificity [11]. Brain MRI with contrast is indicated as a diagnostic complement if there is a suspicion of metastasis in brain CT with contrast or, initially, in patients with neurological symptoms or in stage II-IV NSCLC candidates for curative treatment [1]. Positron emission tomography (PET) with fluorodeoxyglucose (FDG) can be used in addition to previous exams to assess the presence of metastases, especially in the mediastinal location, in patients eligible for radical surgery [11]. PET-CT has proven significantly useful both in characterizing the solitary lung nodule and in preoperative and post-treatment staging, thanks to its high negative predictive value, except for nodules <1cm and those with a "ground-glass" appearance [13-15]. Moreover, the uptake of radiolabeled glucose can be localized, highlighting any heterogeneity within the tumor masses and consequently biopsy suspicious areas with high glucose

metabolism with a higher probability of reaching a diagnostic result. 18F-FDG PET-CT allows for more precise lung cancer staging than CT, mainly due to its higher sensitivity in detecting extrathoracic and bony metastases [16-19]. The use of invasive methods, such as endoscopic ultrasound and, in case of negativity, mediastinoscopy, is recommended by ACCP and EST/ERS guidelines in the presence of specific requirements, even in cases of mediastinal lymph nodes negative on CT and PET-CT evaluations [20,21]. These requirements include tumor size >3cm, central tumor, and the presence of ipsilateral hilar lymph node metastases, motivated by patients with these characteristics having a higher risk of occult metastases in the mediastinal lymph nodes [21]. These invasive methods are also necessary for patients where evidence of mediastinal non-bulky lymphadenopathy on PET-CT represents the only obstacle to radical "up-front" surgical treatment. In this case, mediastinal involvement needs confirmation through endoscopic ultrasound, as false positives on PET-CT can reach 20% of cases [21].

1.4.3 Disease diagnosis/staging

The choice of the most suitable invasive procedure for the histological typing of cancer depends on the location of the primary tumor (central or peripheral), the growth pattern concerning the airways (endobronchial or peribronchial), and the presence or absence of mediastinal and/or distant lymph node metastases [22]. Central lesions, visible endoscopically or located in the inner third of the lung, are mostly typed through fiber optic bronchoscopy, a method that allows for a diagnosis in approximately 90% of cases [22,23]. In cases where the neoplasm extends into the tracheal or bronchial lumen, it can be biopsied using standard flexible forceps or, if the lesion appears extensively necrotic on the surface, with transbronchial needles (TBNA) to obtain material from the depth of the lesion. If, on the other hand, the neoplasm does not extend into the airways, i.e., with a peribronchial/esophageal pattern, it can be approached through endobronchial ultrasound (EBUS) or transesophageal ultrasound (EUS) [24-26]. Additionally,

bronchial washing and brushing can be performed during bronchoscopy for cytological examination [11].

Peripheral lesions, not visible endoscopically, can be biopsied through bronchoscopy, thanks to the current availability of sophisticated methods for guiding bronchoscopic sampling, such as radial ultrasound, electromagnetic navigation, virtual bronchoscopic navigation, and core beam CT. Positive predictive factors for the success of this approach include the radiological "bronchus sign" (a sign indicating the presence of a bronchus/bronchiole terminating within the lesion), lesion size >2 cm, and a solid pattern. However, even with these positive predictive factors and the most modern guidance techniques, the bronchoscopic approach allows for a diagnosis in only about 70% of cases [[27]. For this reason, the transthoracic percutaneous CT-guided approach (TTNA) can be used, a technique that achieves a diagnostic yield of about 90%, with a higher risk of pneumothorax, especially in cases of very peripheral lesions smaller than 2 cm and with a ground-glass appearance [28,29].

Currently, in the presence of potentially pathological mediastinal adenopathies detected on CT or PET-CT, endoscopic ultrasound with ultrasound can be used to type the disease by biopsying these lymph nodes, with the advantage of high diagnostic success and a low rate of complications, especially in patients with advanced disease with a peripheral primary lesion and a significant risk of pneumothorax in case of percutaneous biopsy [20,30].

More invasive surgical and diagnostic procedures can be used if there is no way to access the neoplasm or lymph nodes with the abovementioned methods. These include mediastinoscopy, which provides access to paratracheal, tracheobronchial, and anterior subcarinal lymph nodes; anterior parasternal mediastinotomy, indicated for tumors in the upper left lobe to exclude the presence of metastatic lymph nodes in the left mediastinum, hilum, and aortopulmonary window; and video-assisted thoracoscopy, through which it is possible to biopsy lymph node stations not accessible with the methods above and evaluate the possible presence of pleural metastases [11].

Currently, for mediastinal staging in potentially operable NSCLC patients, between endoscopic ultrasound and mediastinoscopy, the AIOM guidelines favor

endoscopic ultrasound as the first-choice option [1]. Finally, in the case of suspected "superficial" metastases highlighted by CT and/or PET-CT, there is the possibility of effectively, safely, and less invasively sampling them through external ultrasound guidance [31].

1.4.4 Staging According to the TNM System

The staging of lung carcinoma according to the TNM system is universally the most accepted and applied means of defining the anatomical extent of the neoplasm through the definition of three parameters: T (primary tumor extension), N (lymph node involvement), and M (presence or absence of distant metastases). Combining these parameters makes it possible to define four stages, allowing clinical practice to estimate prognosis and determine the most appropriate therapeutic approach for each stage [11,32-36].

1.5 Molecular Predictive and Prognostic Biomarkers

The molecular characterization of lung cancer, in particular non-small cell lung cancer (NSCLC), is an essential pillar for accurate diagnostic and therapeutic framing, as the existence of disease subtypes where the pathogenetic process is driven by specific mutations (oncogene-addicted disease) is well-known. These mutations are targetable through biological drugs that can improve survival [11]. In all patients with NSCLC not eligible for locoregional treatments, performing a baseline panel to search for these mutations is indicated. This includes mutations in EGFR (Epidermal Growth Factor Receptor) and BRAF (B-Raf proto-oncogene), translocations involving ALK (Anaplastic Lymphoma Kinase), ROS-1 (Proto-oncogene tyrosine-protein kinase ROS), and NTRK 1, 2, and 3 (Neurotrophic Tyrosine Receptor Kinase), as well as the evaluation of PD-L1 (Programmed-death ligand 1) expression levels [37,38]. Patients with adenocarcinoma (ADC), large cell carcinoma (LCC), mixed NSCLC with ADC, and NSCLC not otherwise specified (N.A.S.) are more likely to have these mutations. They should undergo this type of mutational analysis.

Additionally, testing for EGFR mutations is recommended for young or non-smoker patients with squamous cell carcinoma. Cases where squamous histology is diagnosed on small tissue biopsies or cytological samples, and a mixed adeno/squamous component cannot be excluded should be tested for both EGFR and BRAF mutations [39,40]. These analyses can be performed on surgical specimens, biopsies, or cytological samples of the primary tumor and/or metastasis [40]. In cases where standard lung biopsy does not provide sufficient material, selected patients may undergo mutation testing on circulating tumor DNA (ctDNA) extracted from peripheral blood [1].

Activating mutations in the EGFR gene are more commonly found in patients with adenocarcinoma, females, non-smokers, and Asian descent. Mutations in exons 18, 19, and 21 are considered sensitizing mutations, predicting a response to first-generation (gefitinib and erlotinib), second-generation (afatinib and dacomitinib), and third-generation (osimertinib) EGFR tyrosine kinase inhibitors. Conversely, mutations in exon 20 are associated with resistance to these inhibitors [11,41-45].

Point mutations V600 in exon 15 of the BRAF gene, with the most frequent being responsible for the valine-to-glutamate substitution (p.V600E), have recently received approval as positive predictive biomarkers for response to simultaneous treatment with the tyrosine kinase inhibitors trametinib and dabrafenib [39].

ALK oncogene translocations allow access to treatment with ALK tyrosine kinase inhibitors of the first (crizotinib), second (alectinib, ceritinib, and brigatinib), and third generation (lorlatinib) [46-50]. Chromosomal rearrangements of the ROS1 oncogene allow access to treatment with ROS1 tyrosine kinase inhibitors of the first (crizotinib) and second generation (entrectinib) [51,52]. Although rarer than other alterations, chromosomal rearrangements of the NTRK 1, 2, and 3 genes should still be tested due to the possibility of accessing treatment with entrectinib [53].

Finally, evaluating PD-L1 expression is essential for selecting patients eligible for first-line immunotherapeutic treatment with pembrolizumab [54].

1.6 NSCLC Treatment

The choice of the most appropriate treatment path for patients with NSCLC is based on prior adequate staging and the prognostic factors of each patient [11]. Three major groups of diseases can be distinguished, each following a different treatment path: early-stage disease, locally advanced disease, and progressive disease [1].

1.6.1 Treatment of Early-Stage Disease

In this subset of patients, radical-intent surgery represents the first-choice treatment, as it is both the most effective and the only option capable of enabling cure [11]. The type of intervention depends on the patient's overall condition and the stage of the disease. Specifically, it is feasible if the disease is potentially resectable (Stage I, II, and Stage IIIA/IIIB in selected cases) and the patient's pulmonary reserve is sufficient to guarantee adequate respiratory function postoperatively. Therefore, patients eligible for resection undergo a thorough assessment of cardiorespiratory function before the procedure [1] [11]. Currently, various surgical options exist, including lobectomy with associated hilar-mediastinal lymphadenectomy—considered the treatment of choice and indicated when the neoplasm involves a single lobe with a healthy margin of the proximal bronchus of at least 1 cm and in the absence of lymph node metastasis. Other options include anatomical segmentectomy, acceptable only for early stages; lobectomy with reconstructive procedures such as bronchoplasty (sleeve lobectomy), recommended in cases of involvement of the main bronchus; and pneumonectomy, employed when the lesion is not accessible by other methods above or in the presence of significant trans-scissure extension [1,11]. Thanks to technological progress, minimally invasive surgery, such as video-assisted thoracoscopic or robotic surgery, has recently become a valid alternative to thoracotomy in Stage I [55-57].

An alternative to surgery for inoperable patients (T1-2N0) due to medical contraindications, comorbidities, or personal choice is stereotactic radiotherapy, preferable for its efficacy over conventional radiotherapy [58,59].

Considering the high incidence of disease recurrence after radical surgery, adjuvant chemotherapy is currently considered the standard treatment for adequately selected Stages II-III. Specifically, chemotherapy with cisplatin-based regimens is the first-choice therapeutic option [11,60,61]. Neoplasms in this category are highly heterogeneous and complex, and therapeutic decisions are preferably managed by a multidisciplinary team [1]. Possible treatments vary based on the resectability of the disease, depending on the extent of the primary tumor, the level of lymph node involvement, and the response to any neoadjuvant therapies [1].

Possible therapeutic pathways for resectable locally advanced disease include surgery followed by adjuvant chemotherapy, neoadjuvant platinum-based chemotherapy followed by surgery, and neoadjuvant chemoradiotherapy followed by surgery [1,62,63]. To reduce local recurrences after apparently radical interventions or in cases where involvement of mediastinal lymph nodes emerges postoperatively (pN2), postoperative radiotherapy is a viable option [64].

Multimodal treatment is always indicated in the case of unresectable locally advanced disease (Stage IIIA/IIIB non-resectable or IIIC). In patients with Stage IIIB (N3) or IIIC NSCLC, it is advisable, before initiating treatment, to assess the presence of targetable molecular alterations, similar to Stage IV, to proceed with the most suitable therapeutic approach [1]. In patients in good general condition (ECOG PS 0-1), concurrent treatment with radical-dose platinum-based chemoradiotherapy should be considered as the first-choice therapeutic option [65].

Finally, in patients with unresectable Stage III disease, in response to or stability of the disease after radical-dose chemoradiotherapy, and with PD-L1 expression on tumor cells greater than or equal to 1%, consolidation therapy with durvalumab for 12 months is strongly recommended as the first-choice therapeutic option [66].

1.6.2 Treatment of Advanced Disease

To date, the treatment choice in patients with advanced-stage NSCLC, i.e., stage IIIB/IIIC not amenable to locoregional treatments and Stage IV, requires a careful

evaluation of parameters such as histology (squamous or non-squamous), PD-L1 expression percentage, the presence of targetable molecular alterations, and the patient's clinical characteristics (age, comorbidities, and performance status) [1]. The disease can be distinguished into oncogene-addicted and non-oncogene-addicted based on the presence of molecular driver alterations, and these distinct entities follow different therapeutic approaches [1].

Oncogene-addicted diseases, depending on the type of molecular alteration, are treated with tyrosine kinase inhibitors, as discussed in Chapter 1.5. In Italy, tyrosine kinase inhibitors targeting EGFR, ALK, ROS1, BRAF, and NTRK are approved and reimbursed. However, broad molecular characterization may lead to identifying other targetable molecular driver alterations with drugs subject to clinical trials or compassionate use [1].

Regarding the treatment of non-oncogene-addicted diseases, the main first-line therapeutic approaches are monoimmunotherapy, immunotherapy combined with chemotherapy, or chemotherapy alone.

In patients with advanced-stage NSCLC, without targetable mutations, with PD-L1 expression ≥ 50%, the first-choice treatment, preferable to chemotherapy, is represented by pembrolizumab, cemiplimab and atezolizumab. This is due to its extension of progression-free survival and overall survival compared to chemotherapy and a lower risk of adverse events (except for immune-related adverse events) [67-69]. In patients with advanced-stage, non-squamous histology, without targetable mutations, with PD-L1 expression < 50%, and with good performance status (0-1), the currently best therapeutic option is the combination of platinum-based chemotherapy, pemetrexed, and pembrolizumab, followed by maintenance therapy with pemetrexed and pembrolizumab after a response or stability of the disease [70].

In patients with advanced-stage, squamous histology, PD-L1 expression < 50%, and good performance status (0-1), the recommended treatment is the combination of carboplatin, paclitaxel or nab-paclitaxel, and pembrolizumab, followed by maintenance therapy with pembrolizumab in case of response or stability of the disease after four treatment cycles [71]. More recently, the combination of nivolumab plus ipilimumab (anti-CTLA4) and platinum-based

short-course chemotherapy was approved as an upfront treatment choice in patients with advanced NSCLC regardless of their PD-L1 expression levels [72].

A possible alternative for patients suitable for chemotherapy as first-line therapy due to absolute or relative contraindications to immunotherapy and affected by non-squamous histology in locally advanced or metastatic stage is the combination of cisplatin and pemetrexed. This is due to similar efficacy and better tolerability compared to cisplatin and gemcitabine combination [73]. After completing first-line chemotherapy in patients with non-squamous histology, free from progression and with good performance status (0-1), if contraindications to immunotherapy persist, maintenance therapy with pemetrexed can be considered. However, careful evaluation is required due to increased toxicity [74,75].

In cases where the disease progresses despite first-line treatment, in patients initially treated with pembrolizumab monotherapy due to PD-L1 expression > 50%, the following therapeutic option is platinum-based chemotherapy [1]. In remaining cases, i.e., patients with PD-L1 < 50%, initially treated with chemotherapy and pembrolizumab, the reference second-line drug is docetaxel, regardless of histology [76,77]. In patients progressing without receiving first-line immunotherapy, compared to second-line chemotherapy, consideration should be given to immunotherapy with nivolumab, atezolizumab, or pembrolizumab (the latter only if PD-L1 ≥ 1%) [78-81].

In the specific case of locally advanced, locally recurrent, or metastatic adenocarcinoma after first-line chemotherapy, the use of nintedanib in combination with docetaxel is approved in Italy. This should be considered, especially in patients progressing within the first nine months of first-line therapy [82,83].

Finally, a separate consideration is needed for elderly patients and those with poor performance status. Vinorelbine monotherapy significantly prolongs overall survival compared to supportive care alone. On the contrary, combining multiple third-generation agents (gentamicin and vinorelbine) does not show advantages over monotherapy [84]. It should be noted that populations of elderly and/or performance status two patients are heterogeneous. Through careful selection to reduce the risk of excessive toxicity, platinum-based chemotherapy regimens can

be used at [1]. In patients with performance status 3 and 4 with non-oncogene-addicted disease, supportive care is indicated [1].

1.7 Immunotherapy approach in lung cancer

1.7.1 Overview and Mechanism

1.7.1.1 Immunosurveillance and Biological Bases for Immunotherapy

The immune system inherently performs immunosurveillance, recognizing and eliminating transformed cellular clones before they give rise to neoplasms. This daily process involves cancer-immunity cycles consisting of seven phases: release of tumor antigens due to neoplastic cell death, presentation of these antigens to T cells by antigen-presenting cells (APCs), T cell activation (priming phase), migration, infiltration, recognition of tumor cells, and ultimately, their attack and elimination (effector phase) [85]. However, neoplastic cells possess mechanisms to evade the immune system, and the immune response exerts selective pressure, promoting the development of clones with reduced immunogenicity, a process known as tumor immune editing [86].

Considering these mechanisms, attention has shifted from the tumor to the host's immune system. The aim is to develop therapies that recruit immune cells to recognize and eliminate neoplastic cells, exploiting the adaptive immune system's memory for long-term survival, which is impossible with conventional cytotoxic therapies [120]. Initial attempts at immunotherapy were conducted in the 1960s and 1970s when these immunological anti-tumor defense mechanisms had yet to be proven. These innovative approaches involved nonspecific immunomodulating agents such as Bacillus Calmette-Guérin or levamisole [11]. In the 1980s, thanks to biotechnological advances, a more selective process became possible. In the last two decades, the use of monoclonal antibodies targeting specific checkpoints, including cytotoxic T-lymphocyte antigen 4 (CTLA-4), programmed death-1 (PD-1), and its ligand PD-L1, became a crucial therapy known as immune checkpoint blockade (ICB) [11].

Other immunotherapeutic approaches developed over the years include vaccination with tumor antigens, passive immunotherapy with antibodies, and using tumor-specific or engineered T lymphocytes expressing chimeric antigen receptors (CAR) [87].

1.7.1.2 Mechanism of Action of Immune Checkpoint Inhibitors (ICIs)

The activation of T cells requires the presentation of antigens by major histocompatibility complex (MHC) molecules on antigen-presenting cells (APCs) to the corresponding T cell receptor (TCR) of naïve T lymphocytes [86]. Full activation requires costimulatory interaction between CD28 molecules on lymphocytes and B7-1 and B7-2 molecules on APCs. Inhibitory checkpoints finely regulate this process to prevent activation in inappropriate contexts and autoimmunity while regulating responses to microorganisms [86]. One inhibitory checkpoint is CTLA-4, expressed by activated effector T cells and regulatory T cells (Tregs). It competitively inhibits CD28 by reducing the availability of B7 molecules, with an affinity for B7 10 to 20 times higher than that of CD28, inhibiting lymphocyte proliferation and interleukin-2 (IL-2) secretion [88]. Another checkpoint receptor expressed by activated T cells is PD-1, which recognizes two ligands: PD-L1, usually defined by APCs and many other cells, and PD-L2, primarily represented by APCs. PD-1 binding to its ligands recruits cytoplasmic tyrosine phosphatases responsible for turning off signals transmitted by the TCR complex, resulting in lymphocyte inactivation [86]. Physiologically, these molecules are necessary for immune response control. PD-1 plays a crucial role in terminating effector responses of T lymphocytes, especially CD8+, in peripheral tissues, while CTLA-4 limits the initial activation of T lymphocytes in secondary lymphoid organs [86].

Neoplastic cells exploit these inhibitory molecules to evade anti-tumor responses. Studies on murine and human models have shown that CTLA-4 and PD-1 are frequently overexpressed in tumor-infiltrating T lymphocytes, which often exhibit altered effector functions, presenting a phenotype defined as exhausted. This is likely due to tumor antigens being presented by APCs in a context lacking a

robust innate immune response, resulting in low levels of costimulatory B7 molecules sufficient to bind CTLA-4 but not CD28. Additionally, neoplastic cells often express increased levels of PD-L1 due to gene amplification [86].
Blocking these inhibitory molecules using monoclonal antibodies against CTLA-4, PD-1, and PD-L1 can enhance anti-tumor immune responses [86]. Anti-CTLA-4 antibodies act during antigen presentation, inhibiting the CTLA-4 and B7 interaction, leading to increased CD28 and B7 binding and consequently reactivating T lymphocytes [89]. Moreover, since CTLA-4 is also expressed by Tregs, blocking their immunosuppressive activity is an added benefit [90]. Anti-PD-1 and anti-PD-L1 antibodies act during the effector phase of the cancer-immunity cycle, preventing the binding of PD-L1 expressed on neoplastic cells to PD-1 on effector T lymphocytes, thus preventing their inactivation [91].

1.7.2 Predictive and Prognostic Factors for Immunotherapy Response

Despite confirmed efficacy in various studies, the response rate to ICIs is unfortunately not as high as that of targeted therapies. The definition of predictive and prognostic biomarkers is more complex. [92] and, to date, the only validated and reliable biomarker is represented by the immunohistochemistry (IHC) expression of PD-L1.

1.7.2.1 PD-L1 as a Predictive Biomarker for Therapeutic Efficacy

PD-L1 is currently the most widely used biomarker in clinical practice. Expression percentages of this molecule correlate with therapy response, especially in patients with PD-L1 ≥ 50%. Those with very high levels (≥ 90%) show a better response rate than those with expression levels of 50%-89%, along with improved progression-free survival [93]. Several studies have demonstrated that upregulation of PD-L1 is associated with increased efficacy of pembrolizumab and other ICIs in monotherapy and combination therapies [94-96]. However, this correlation is not always respected due to tumor cell heterogeneity and the involvement of immune evasion mechanisms independent

of PD-1/PD-L1. Thus, PD-L1 is considered an incomplete biomarker, highlighting the need for additional complementary biomarkers [92].

1.7.2.2 Laboratory Methods for PD-L1 Evaluation

PD-L1 expression assessment is performed using IHC with antibodies validated for formalin-fixed, paraffin-embedded, or cytological samples prepared as cell blocks. The quantitative parameter for sample adequacy is a minimum of 100 neoplastic cells. The validated interpretation method is the tumor proportion score, based on the percentage assessment of PD-L1 positivity on the surface of neoplastic cells. This is crucial for clinically relevant cutoffs for treatment, i.e., ≥ 50% for first-line ICI use and ≥ 1% for second-line ICI use [54].

1.7.2.3 Other Potential Markers

Another potential, albeit debated, biomarker is the total number of genetic mutations in neoplastic cells, known as "tumor mutation burden" (TMB). Mutated genes produce mutated proteins, which can be recognized as "non-self" by the immune system. Hence, neoplasms with a higher TMB may exhibit a more effective response to ICI therapy. Elevated TMB is typically observed in smokers, and the relatively higher efficacy of immunotherapy in these patients is hypothesized to be linked to the higher TMB [97]. In other neoplasms, such as advanced gastric carcinoma, the potential antitumor role of tumor-infiltrating lymphocytes (TILs) has been highlighted. The KEYNOTE-061 study demonstrated that pembrolizumab's effect could be predicted by the Combined Positive Score, which evaluates PD-L1-positive cells among tumor cells, lymphocytes, and macrophages divided by the total number of tumor cells multiplied by 100 [98]. Identifying additional predictive factors is crucial for anticipating immunotherapy efficacy, as both PD-L1 and TMB, while useful in case selection, may not cover all potential mechanisms of resistance [92].

1.7.3 Primary, Adaptive, and Acquired Resistance to Immunotherapy

Despite achieving unprecedented rates of durable responses, many patients do not benefit from immunotherapy, and progression is common in responders during or after treatment. This is attributed to three forms of resistance: primary resistance, where the tumor does not respond to immunotherapy; adaptive resistance, where the immune system recognizes the cancer but adapts to protect itself; and acquired resistance, where a tumor that initially responded to immunotherapy relapses and progresses after a certain period. The dynamic nature of the immune response, influenced by patient environmental and genetic factors, as well as therapeutic interventions, must be emphasized. While resistance can manifest with varying timelines, the underlying mechanisms are often similar or overlapping [120].

1.7.3.1 Primary and Adaptive Resistance to Immunotherapy

Elements contributing to resistance mechanisms can be categorized as intrinsic and extrinsic mechanisms. In addition to PD-L1 expression, innate mechanisms include:

- Signaling through the mitogen-activated protein kinase (MAPK) pathway and/or loss of PTEN expression, leading to increased PI3K signaling, resulting in the production of VEG-F and IL-8, cytokines inhibitory to T cell recruitment and function.
- Stabilization of β-catenin with consequent constitutive WNT signaling.
- Loss of interferon-gamma (IFNγ) signaling pathways through downregulation or mutation of molecules like signal transducers and activators of transcription (STAT), JAK1/2, and IFNγ receptor chains, potentially a consequence of immunoediting.
- Lack of T cell recognition due to loss of tumor antigen expression. These mechanisms, collectively by expressing or suppressing specific genes and cellular pathways, hinder immune cell infiltration or function within the tumor microenvironment, interfering with antigen presentation mechanisms and conferring resistance to ICI therapy.

- Extrinsic mechanisms, on the other hand, involve various elements of the tumor microenvironment:
- Regulatory T cells (Tregs) suppress the effector activity of T cells through direct contact or by secreting inhibitory cytokines such as IL-10, IL-35, and TGF-β.
- Myeloid-derived suppressor cells (MDSCs) promote angiogenesis, tumor invasion, metastasis, and immunosuppression.
- Tumor-associated macrophages (TAMs) with pro-tumorigenic properties.
- Other inhibitory immune checkpoints, such as increased expression of TIM-3 (T-cell immunoglobulin and mucin domain-containing protein 3) by T cells[86].

1.7.3.2 Acquired Resistance to Immunotherapy

One significant advantage of immunotherapeutic treatment is the potential for long-lasting responses. However, it is not uncommon for patients who initially responded for a certain period to experience progression due to mechanisms leading to acquired resistance to ICI therapy. These mechanisms include the loss of T cell function, lack of T cell recognition through downregulation of tumor antigen presentation, and the development of "escape" mutations in the tumor. These processes can occur according to the mechanisms described earlier. If antitumor T cells were to change their functional phenotype, no longer exerting cytotoxic activity, a patient who initially responded to immunotherapy would experience recurrence.

Additionally, given the specificity of T cells to tumor neoantigens, neoplastic cells may develop acquired resistance through decreased expression or mutations of these antigens, possibly through epigenetic modifications. However, the existence of such mechanisms in clinical settings has yet to be confirmed thus far [86].

1.7.4 LIPI Score (Lung Immune Prognostic Index)

Considering the need for new predictive and prognostic markers for immunotherapy response, a recently developed prognostic index called the LIPI score (Lung Immune Prognostic Index) focuses on blood levels of lactate dehydrogenase (LDH) and the derived neutrophil-to-lymphocyte ratio (dNLR) [99]. The development of the LIPI score is based on the demonstrated correlation of these parameters with ICI treatment response in melanoma patients and numerous previous studies investigating systemic inflammation as a mechanism of immunoresistance. Various routine blood parameters, including elevated concentrations of circulating leukocytes, absolute neutrophil count, platelet count, LDH levels, neutrophil-to-lymphocyte ratio (NLR), and the derived neutrophil-to-lymphocyte ratio (dNLR), have been explored as possible inflammatory biomarkers in cancer patients due to their accessibility through a simple complete blood count. Among these, elevated LDH levels in patients with lung cancer treated with chemotherapy or molecularly targeted therapy have been associated with decreased survival when increased 1 to 2.5 times above the upper limit of normal (ULN). Regarding neutrophils, it has been recently demonstrated that the pro-inflammatory state induces "emergency granulopoiesis," increasing the rate of neutrophil generation and releasing poorly differentiated and immature cells into circulation, with subsequent pro-tumoral effects. The NLR represents a valid parameter in measuring this inflammatory state and is a prognostic factor in NSCLC patients. However, the dNLR (the absolute neutrophil count / [total leukocyte count - absolute neutrophil count]) may be even more significant, as it includes monocytes and other granulocytic subpopulations. The LIPI score considers a dNLR greater than three and an LDH value higher than the upper limit of normal (ULN). Based on the presence of none, one, or both of these factors, three prognostic groups can be identified: "good" (0 factors), "intermediate" (1 factor), and "poor" (2 factors). A reverse proportional correlation has been demonstrated between the LIPI score and overall survival (OS), irrespective of histological subtype and patient age, along with a correlation with progression-free survival (PFS) and disease control rate in patients treated with ICIs. Notably, a pre-treatment LIPI of "poor" type is associated with worse outcomes in patients

treated with ICIs, suggesting the potential utility of this tool in identifying patients who may or may not benefit from immunotherapy [99].

1.8 MDSCs (Myeloid-Derived Suppressor Cells)

1.8.1 Discovery, General Overview, and Classification

1.8.1.1 Discovery and Mechanisms Underlying the Genesis of MDSCs

The term "myeloid-derived suppressor cells" was first introduced in the literature over 15 years ago to define an unspecified group of myeloid cells with potent immune regulatory activity [100]. Myeloid cells are essential to the healthy innate immune system for pathogen elimination and tissue remodeling. Under physiological conditions, myelopoiesis and the differentiation of granulocytes and macrophages are controlled by cytokines such as GM-CSF, G-CSF, and M-CSF [100]. However, in cancer and other pathological conditions, myeloid cells are reprogrammed through the overproduction of these factors, promoting the generation of MDSCs [101,102]. This process is linked to the activation of myeloid cells [100]. The classical activation of these cells occurs in response to solid signals, primarily through Toll-like receptors (TLR), DAMPs, and PAMPs, leading to the recruitment of monocytes and neutrophils from the bone marrow, increased phagocytosis and respiratory burst, release of proinflammatory cytokines, and upregulation of major histocompatibility complex (MHC) class II and costimulatory molecules [103,104]. This response is usually short-lived and ends with eliminating the threat [100]. In unresolved inflammation, as in the case of cancer and other chronic conditions, these activating signals persist but become relatively weak [100,105]. Neutrophils and monocytes produced under these conditions exhibit an immature phenotype, relatively weak phagocytic activity, increased production of reactive oxygen species (ROS) and nitric oxide (NO), and high expression of arginase, PGE2, and various anti-inflammatory cytokines. These characteristics are absent in classically activated cells, defining a state of pathological activation capable of inhibiting the immune response and supporting

tumor progression—both distinctive features of MDSCs [100,106,107]. The longer these conditions persist, the greater the pathological activation of MDSCs, resulting in a heterogeneous cellular population in tissues composed of classically activated neutrophils, monocytes, and pathologically activated cells [100]. For example, in the early stages of neoplasia development, true immunosuppressive MDSCs are rare. However, MDSC-like cells with common biochemical and genomic characteristics likely represent an intrinsic phase of their development [108,109]. This pathological activation could be transferred through hematopoietic progenitors, serving as a kind of innate immune memory through epigenetic modifications and signals that modulate the activity of transcription factors [109].

The accumulation of MDSCs is, therefore, a complex and gradual phenomenon governed by multiple factors that, for simplicity, can be divided into two groups [110]. The first group of signals is necessary to expand immature myeloid cells and includes factors produced by tumor cells or bone marrow stromal cells in response to chronic inflammation. This includes GM-CSF, G-CSF, M-CSF, S-SCF, VEGF, and polyunsaturated fatty acids [111-114]. Other factors involved in this process include the adenosine A2b receptor, the cytoplasmic NLRP3 receptor, retinoblastoma protein (RB1), S100A9 and S100A8 alarming, anti-apoptotic molecules c-FLIP and MCL-1, and transcription factors/regulators STAT3, STAT5, IRF8, C/EBP-β, and NOTCH [115,116]. The second group of factors is responsible for the pathological activation of MDSCs, mediated by inflammatory cytokines and DAMPs, including IFN-γ, IL-1β, IL-4, IL-6, IL-13, TNF, and HMGB1, which signal mainly through NF-kB, STAT1, and STAT6 [116].

1.8.1.2 Phenotypic Classification and Subpopulations of MDSCs

Three subpopulations of MDSCs can be distinguished in humans: polymorphonuclear MDSCs (PMN-MDSC), monocytic MDSCs (M-MDSC), and immature MDSCs (i-MDSCs) lacking typical markers of PMN-MDSCs or M-MDSCs [117]. However, this subdivision is simplistic, as it is now demonstrated that the MDSC population is widely heterogeneous [118]. In mice, PMN-MDSCs are defined by surface expression of CD11b and Ly6G and low levels of Ly6C,

while in humans, they are positive for CD11b, CD15, and CD66b and negative for CD14; they are the most represented MDSC subpopulation in all types of neoplasia and share some morphological characteristics with neutrophils [119]. M-MDSCs are characterized by the expression of CD11b, high levels of Ly6C, and low levels of Ly6G in mice and the expression of CD14 and negativity or low levels of HLA-DR in humans [108]. Additionally, M-MDSCs can differentiate into macrophages capable of suppressing T cell activation in vitro, similar to tumor-associated macrophages (TAMs) [120].

Moreover, these MDSC subpopulations exert their functions through partially different mechanisms [118]. PMN-MDSCs produce large quantities of free radicals and require cellular contact to exercise their specific immunosuppressive effects. In contrast, M-MDSCs predominantly produce NO and immunosuppressive cytokines, molecules with paracrine effects, requiring only cellular proximity to exert their impact [118].

1.8.1.3 Immunosuppressive and Pro-Tumoral Functions of MDSCs

MDSCs possess potent suppressive activity against anti-tumor immunity, primarily exerted through inhibiting T lymphocyte functions via various mechanisms and inhibitory receptors [118]. Within the tumor microenvironment (TME), MDSCs express high levels of Fas ligand (FasL). Through the FasL-Fas axis, they induce apoptosis of tumor-infiltrating CD8+ T lymphocytes, resulting in the local suppression of their cytotoxic functions [118]. These cells can also induce immunosuppression through the use of inhibitory checkpoints PD-1, CTLA-4, and TIM3, given their ability to express PD-L1 and galectin-9, which respectively bind to PD-1 and TIM3 on TILs, limiting their anti-tumor activity [118]. MDSCs produce elevated quantities of IL-10 and TGF-β [118]. IL-10 interferes with the function of CD8+ T cells in various types of tumors, is implicated in the development of Tregs, and is associated with reduced levels of IL-12, a cytokine secreted by DCs involved in stimulating anti-tumor immunity [121-123]. TGF-β hinders the proliferation of effector T cells by inhibiting the production of IL-2 and directly suppresses the cytotoxic function of CD8+ T

lymphocytes by inhibiting the expression of genes encoding IFN-γ, granzyme B, and perforin [124-126].

Another immunosuppressive mechanism is the ability of MDSCs to exploit the adenosinergic pathway, made possible by the high expression of ectonucleotidases CD39 and CD73 [118]. These are induced by hypoxia-inducible factor-1α (HIF-1α) under hypoxic conditions within the TME, converting ATP to adenosine, a molecule capable of functionally inhibiting CD4+ and CD8+ T cells and stimulating regulatory cells [127,128]. HIF-1α upregulation in response to hypoxia also promotes the overproduction of inducible nitric oxide synthase (iNOS) and arginase 1 (Arg1), both enzymes that use L-arginine as a substrate [129]. This leads to L-arginine depletion in the TME, resulting in the cell cycle arrest of T lymphocytes by silencing cyclin D3 and the loss of CD3ζ expression, a component of the TCR, preventing signal transduction and causing T cell dysfunction [130-132].

Another enzyme expressed at high levels by MDSCs is indoleamine 2,3-dioxygenase 1 (IDO1), which causes depletion of L-tryptophan within the TME and the production of kynurenine, leading to the accumulation of its lymphotoxic metabolites [133,134]. Tryptophan deficiency also activates "general control nonderepressible 2" (GCN2) kinase, inducing the downregulation of CD3ζ in CD8+ T cells and cell cycle arrest with subsequent anergy [135,136]. Additionally, it inhibits the activation of mammalian target of rapamycin (mTOR) and protein kinase C (PKC), triggering autophagy in effector T cells and enhancing Treg function [137,138]. Kynurenine exerts its action by binding to the aryl hydrocarbon receptor (AhR) on dendritic cells and macrophages, promoting their differentiation into a regulatory phenotype, thus facilitating the transdifferentiation of Th17 lymphocytes and naive CD4+ T lymphocytes into Tregs through the induction of FoxP3 expression [139]. Furthermore, downstream signaling events of AhR activation in CD8+ T cells modulate PD-1 expression [140].

MDSCs can generate free radicals through various mechanisms [118]. Among these, the production of S100A8 and S100A9 proteins, binding calcium, contributes to increased ROS production through enhanced NADPH oxidase

activity, generating superoxide anions O2-, which, in the presence of water, are converted into hydrogen peroxide H2O2, a potent suppressor of T lymphocyte activity [141,142]. In addition to ROS, MDSCs can also mediate the production of peroxynitrite ONOO-, hindering lymphocytic tumor infiltration through the nitration of chemokine CCL2, leaving tumor-specific T cells confined to the surrounding stroma [143,144].

Within the TME, tumor cells induce the activation of cyclooxygenase-2 (COX-2) in MDSCs, leading to the production of various inflammatory mediators, including PGE2, a pro-inflammatory molecule with a dual role, both positive and negative, in terms of anti-tumor immune response. It is noted for its ability to direct myeloid precursors toward a tolerogenic phenotype, resulting in the accumulation of MDSCs and Tregs [145,146].

MDSCs also promote epithelial-mesenchymal transition, a process that transforms polarized epithelial cells into multipotent mesenchymal cells with enhanced metastatic capabilities and resistance to apoptosis [147]. This is made possible by the role of many pro-tumoral factors produced by MDSCs, such as TGF-β, IL-10, IL-6, and VEGF, which, among their functions, can induce a stem-like phenotype in neoplastic cells [148,149].

1.8.1.4 Contribution of MDSCs to Mechanisms of Immunotherapy Resistance

While immunotherapy has allowed for unprecedented rates of durable response in a significant fraction of subjects, a substantial number of patients experience a form of primary or acquired resistance to treatment, and the role of MDSCs in contributing to these phenomena is well-established [86].

In preclinical models of melanoma, it has been demonstrated that MDSCs can diminish the effectiveness of anti-PD-1 and anti-CTLA-4 therapies [205]. Specifically, the neutralization of FasL in combination with anti-CTLA-4 and anti-PD-1 has reduced tumor growth and T lymphocyte apoptosis in tumor-bearing mice compared to those treated with ICIs alone [150]. Blocking the FasL-Fas axis has also proven advantageous in adoptive cell transfer with CD8+ T cells, preventing apoptosis of intratumoral lymphocytes mediated by PMN-MDSCs,

thereby enhancing treatment efficacy [150]. In patients with metastatic melanoma, a correlation has emerged between MDSC levels in peripheral blood and the response to ipilimumab. Specifically, patients with low levels of M-MDSC Lin- CD14+ and HLA-DR- showed a better response to treatment, suggesting the importance of MDSCs as a potential prognostic marker for the efficacy of immunotherapy with ICIs [118,151].

In patients with advanced-stage non-small cell lung cancer (NSCLC) treated with nivolumab, higher baseline levels of PMN-MDSCs were detected in patients progressing compared to those responding to treatment [152]. Therefore, it can be inferred that MDSCs contribute to immunotherapy resistance irrespective of the administered ICI or the type of neoplasm [118].

The specific mechanisms by which MDSCs induce resistance have been investigated in various studies. For example, evaluating the production of NO by MDSCs and the concentration of S100A8/A9 serum proteins in melanoma patients treated with ipilimumab revealed that "non-responders" had elevated levels of both molecules after the first ipilimumab infusion compared to "responders" [153]. Additionally, a significant increase in M-MDSCs in the peripheral blood of "non-responders" was observed, whereas M-MDSC frequencies decreased in "responders" compared to baseline values [153]. Since NO and S100A8/A9 are molecules produced by MDSCs with suppressive activity on antitumor immune response, this could represent one of the mechanisms MDSCs confer resistance to ICI therapy [118].

Another confirmed mechanism by which MDSCs can induce resistance to ICIs is through the TGF-β pathway [118]. In a study analyzing a subset of urothelial tumor patients "non-responsive" to anti-PD-L1 therapy, RNA sequencing revealed an association between TGF-β levels and a poor response to treatment [154]. Using murine models of colon adenocarcinoma (MC38) and mammary carcinoma (EMT6), this study demonstrated that therapeutic blockade of TGF-β with antibodies could promote CD8+ T cell-mediated antitumor immunity, sensitizing neoplastic cells to anti-PD-1 therapy [154]. Specific evidence of how MDSCs are responsible for immunotherapy resistance through TGF-β production emerged by attempting to neutralize this molecule in a murine model with breast cancer (4T1

mammary mouse model), demonstrating that the absence of TGF-β promotes the antitumor activity of T cells in co-culture with MDSCs [155]. Moreover, MDSC depletion reduced the antitumor effects mediated by TGF-β neutralization [155].
In the context of therapy with tumor-specific or engineered T lymphocytes expressing chimeric antigen receptors (CAR), there is abundant evidence that MDSCs, by contributing to the immunosuppressive nature of the tumor microenvironment (TME), can compromise the infiltration and antitumor function of these cells [118].

1.9 c-FLIP (cellular FLICE-inhibitory protein)

1.9.1 Role and Functions of c-FLIP

Cellular FLICE (FADD-like IL-1β-converting enzyme)-inhibitory protein, or c-FLIP, is a central regulator. Activation is inhibited by procaspase cleavage, inhibiting apoptotic signal transduction and promoting cell survival [156]. However, the c-FLIP isoform has a dual role in immune system cells, acting pro- and anti-apoptotic. Whether it acts as an inhibitor or activator of caspase eight depends on various parameters, including cellular context and molecule expression levels. At low concentrations, i.e., physiological levels, c-FLIPL heterodimerizes with procaspase 8 and undergoes processing, leading to activation and apoptosis. Conversely, elevated levels of c-FLIPL make it a competitive inhibitor of procaspases 8 and 10, serving as a potent apoptosis inhibitor [156].

1.9.2 Pathological Role of c-FLIP in Cancer and Immunosuppression

Tumor cells can evade apoptosis through various mechanisms, and resistance to chemotherapy is often linked to the failure of programmed cell death [156]. Increased expression of c-FLIP at the DISC formation level has been demonstrated in various human neoplasms, including ovarian, colon, breast, and prostate cancer, and glioblastoma. It is associated with resistance to apoptosis induced by Fas and TRAIL receptors [156]. Furthermore, an inverse correlation

between c-FLIP expression and susceptibility to chemotherapy has been demonstrated in tolerogenic M-MDSCs in vivo and in vitro [157].

In addition to influencing cell survival, c-FLIP plays a vital role in regulating the homeostatic processes of the immune system. It protects mature T lymphocytes from activation-induced cell death, controls the homeostasis of Treg lymphocytes and their survival against FasL-mediated killing by tumor endothelium, as well as the sensitivity to Fas of monocytes and cells derived from them, such as dendritic cells and macrophages, and their vitality in the bone marrow during normal development [157]. It has also been shown that c-FLIP expression is an essential step for the generation of M-MDSCs in the neoplastic context, probably allowing the prolonged survival of myeloid cells and protecting monocytes and macrophages, enabling them to perform their functions within a hostile inflammatory microenvironment [115]. This is one of many implicated mechanisms, as c-FLIP seems to possess direct immunosuppressive properties, regulating the tolerogenic properties of monocytes through the NF-kB signaling pathway and the production of various cytokines [157]. Considering that other anti-apoptotic proteins, such as Bcl-xL and Bcl-2, cannot activate this molecular program, the immunosuppression associated with c-FLIP in monocytes is probably not solely linked to prolonged survival but to a previously unrecognized immunomodulating function of this protein [157]. Supporting this function, there is evidence that human and murine monocytes modified to express c-FLIP acquire immunosuppressive characteristics capable of limiting T lymphocyte activation, both in vitro and in vivo [157]. Drugs capable of blocking c-FLIP expression selectively eliminate M-MDSCs but not PMN-MDSCs, restoring T lymphocyte functions [157].

Moreover, experiments conducted on transgenic mice have shown that FLIP activation during myeloid differentiation induces severe inflammatory pathology characterized by uncontrolled systemic infiltration of myeloid cells capable of suppressing the activity of B and T lymphocytes [157]. Consistent with its immunoregulatory properties, hyperexpressing c-FLIP monocytes isolated from patients with COVID-19 have shown immunosuppressive functions and have been shown to release high levels of pro-inflammatory cytokines through the

activation of an aberrant FLIP-dependent signal and the signal transducer and activator of transcription 3 (STAT3) pathway [158]. Overall, these data emphasize the contribution of c-FLIP to reprogramming monocytes into MDSCs in various pathological contexts, including neoplasia.

1.9.3 Therapeutic Implications and Perspectives as a Predictive Marker

The overexpression of c-FLIP thus has a dual role: on the one hand, it promotes the immunosuppressive activity of MDSCs, and on the other hand, its activation can fuel a chronic inflammatory syndrome associated with myeloid proliferation and immunosuppression [157]. Therefore, FLIP emerges as a new candidate for controlling chronic inflammation and immune dysfunction associated with cancer. Modulating this molecule may serve as a means to block MDSCs and as a target for developing immunomodulatory drugs to control exaggerated and life-threatening immune responses [157]. It is also essential to highlight the potential role of c-FLIP as a predictive factor. Higher serum levels of IL-6 and hyperexpressing c-FLIP monocytes, CD14+, and PD-L1+ circulating in peripheral blood define patients with ductal pancreatic adenocarcinoma with worse overall survival (OS) and worse disease-free survival (DFS) [157]. Furthermore, the counting of circulating monocytes expressing c-FLIP, in association with specific surface markers induced by it, such as PD-L1, PD-L2, and CD38, may be a valuable tool to improve the understanding of the immunological landscape of cancer patients for more targeted treatment. In the future, targeting hyperexpressing c-FLIP monocytes in combination with immune checkpoint inhibitors (ICIs) could enhance the effectiveness of immunotherapy [157].

1.10 Interleukin-8 (IL-8) and lung cancer

Cytokines and other soluble factors are important in cancer development and treatment responses. For instance, several studies have reported that vascular endothelial growth factor (VEGF) and erythropoietin (EPO) could represent prognostic factors in NSCLC [159]. In particular, CXC chemokines, small

molecules, and secretory peptides are frequently expressed abnormally in cancer patients and have been found to promote cancer progression by facilitating tumor angiogenesis, inflammation, and metastasis [160]. Interleukin-8/CXCL8 (IL-8) is a small proinflammatory cytokine, a member of the CXC chemokine family, with tumorigenic and pro-angiogenic properties, produced by a variety of cells, including tumor cells, stromal cells, and immune cells [161]. IL-8 acts primarily on neutrophils by binding to the CXCR1 and CXCR2 receptors on their surface, inducing various cellular responses, including chemotaxis, degranulation, and phagocytosis [161].

The role of IL-8 in the development and progression of cancer has been hypothesized in various contexts. For instance, IL-8 has been shown to promote cancer cell growth by activating intracellular signaling pathways such as the mitogen-activated protein kinase (MAPK) pathway and phosphatidylinositol 3-kinase (PI3K) pathway, which are involved in increased cell proliferation, cell survival, and metabolism [161]. IL-8 also stimulates neoangiogenesis and cancer cell motility and dissemination by stimulating their migration and invasion through the extracellular matrix [162]. Of note, high IL-8 levels have demonstrated a negative prognostic impact in several solid cancers, such as melanoma, renal cell carcinoma, urothelial cancer, and colorectal cancer [163-165].

Nevertheless, despite the increasing attention towards cytokines, particularly in the current era of immunotherapy, the role of IL-8 in lung cancer is still a matter of active research since its exact impact is not yet fully defined.

2. MATERIALS AND METHODS

2.1 Patients and Study Approval

Patients with advanced stage Non-Small Cell Lung Cancer (NSCLC) treated with Immune Checkpoint Inhibitors (ICIs) such as pembrolizumab, nivolumab, and atezolizumab as first or second-line therapy were prospectively enrolled between January 2019 and September 2020 at the Medical Oncology Unit of the University

Hospital of Verona. Retrospectively, patients who experienced disease progression within six months from the first administration of ICIs (after at least six weeks of treatment) were defined as "progressors" (P), while patients who had disease progression during therapy after at least six months of clinical/radiological benefit were described as "non-progressors" (NP) [166,167]. Blood samples were collected from patients before ICI therapy (T0) and after six weeks (T1). All patients provided written informed consent before sample collection to use their clinical and biological data. This study was approved by the local Ethics Committee (Protocol 1839 CESC) and conducted by the Declaration of Helsinki and Good Clinical Practice.

2.2 Flow Cytometry of Immune Subpopulations

Whole blood samples (100µl/tube) were stained for the detection of cell surface markers with anti-HLA-DR-PE, CD14-ECD, CD38-PE-Cy5, CD45-Al700, CD3-A750, CD16-V450, CD4-V500, CD57-FITC, CD4-PE-Cy7, CD14-APC, CD19-V500 antibodies, all from Beckman Coulter Life Sciences (Brea, CA, USA). Samples were stained using the IMMUNOPREP Reagent kit (Beckman Coulter Life Sciences, Brea, CA, USA) and the Workstation PrepPlus 2 (Beckman Coulter Life Sciences, Brea, CA, USA) following the manufacturer's instructions. Peripheral Blood Mononuclear Cells (PBMCs) (1x10^6) were incubated with FcReceptor Blocking reagent (Miltenyi Biotec, Bologna, Italy) and stained with anti-CD14-APCH7, CD16-FITC, HLA-DR-PE-Cy7, CD14-APC-H7, and the LIVE/DEAD™ Fixable Aqua Dead Cell Stain kit (eBioscience, Thermo Fisher Scientific, Waltham, MA, USA). Samples were fixed and permeabilized using the Foxp3/Transcription Factor Staining Buffer Set (eBioscience, Thermo Fisher Scientific, Waltham, MA, USA) and incubated with anti-FLIP (D5J1E, Cell Signaling Technologies, Danvers, MA, USA) and PE-F(ab')2 Donkey anti-Rabbit IgG (BD Biosciences, San Jose, CA, USA). Samples were acquired using FACSCanto II (BD Biosciences, San Jose, CA, USA) and Navios EX (Beckman Coulter Life Sciences, Brea, CA, USA) and analyzed using FlowJo (Tree Star, Inc. Ashland, OR, USA) and Navios EX (Beckman Coulter Life Sciences, Brea,

CA, USA) software. Circulating cell counts (cells/μl) of specific subpopulations were determined by the ratio of flow cytometry data to white blood cell (WBC) counts obtained from the same blood samples.

2.3 Cytokine Detection

Circulating cytokines in frozen plasma samples from NSCLC patients were assessed using an automated immunoassay workflow. IL-1β, IL-8, TNF-α, and IL-6 levels were precisely quantified using the Ella™ technology (Bio-Techne, Minneapolis, MN, USA). Levels of GM-CSF, IFN-γ, IL-12p70, IL-13, IL-18, IL-2, IL-5, IL-10, IL-17A, IL-27, IL-1α, IL-15, IL-1RA, IL-7, CCL11, CXCL1, CXCL10, CCL2, CCL3, CCL4, CCL5, and SDF-1a were measured using the Luminex Performance Assay 3-plex Kit (R&D System Minneapolis, MN, USA) according to the manufacturer's instructions. TNF-β, IL-31, IFN-α, IL-21, IL-22, IL-23, IL-9, and IL-4 levels were assessed using the same technology, but their concentration was below the detection limit for many patients and consequently excluded from the analysis.

2.4 Cell Isolation and Culture

Peripheral Blood Mononuclear Cells (PBMCs) from NSCLC patient blood samples were isolated using Ficoll-Hypaque gradient centrifugation (GE Healthcare, Uppsala, Sweden). PBMCs from healthy donors (HDs) were isolated from the buffy coat (leukocyte-platelet layer) of healthy volunteers (Transfusion Center, University and Hospital of Verona, Verona, Italy) using the same methods. CD14+ monocytes were isolated by immunomagnetic selection (Miltenyi Biotec, Bologna, Italy) following the manufacturer's instructions and, after verifying purity by flow cytometry, were cryopreserved in liquid nitrogen. PBMCs from HDs were stained with one μM CellTrace Violet (eBioscience, Thermo Fisher Scientific, Waltham, MA, USA) in phosphate-buffered saline (PBS) by incubating at 37 °C for 5 minutes, protected from light. Labeled PBMCs were stimulated with 0.6 μg/mL anti-CD3 and 5 μg/mL anti-CD28 (clone OKT-3

and CD28.2, respectively, both from eBioscience, Thermo Fisher Scientific, Waltham, MA, USA) for four days and co-cultured with thawed CD14+ cells derived from NSCLC patients at a ratio of 3:1 (CD14+ cells: PBMCs). Cell cultures were incubated at 37 °C and 8% CO2 in RPMI culture medium lacking L-arginine (Biochrom AG, Berlin, Germany), supplemented with two mM L-glutamine (Euroclone, Milan, Italy), 150 μM L-arginine (Sigma-Aldrich, St. Louis, MO, USA), 10% fetal bovine serum FBS (Superior, Merck, Darmstadt, Germany), 10 U/ml penicillin and streptomycin (Euroclone, Milan, Italy), and 0.1 mM 2-[4-(2-hydroxyethyl)-1-piperazinyl]-ethane sulfonic acid HEPES (Euroclone, Milan, Italy). After co-culture, cells were stained with PE-Cy7-conjugated anti-CD3 (eBioscence, Thermo Fisher Scientific) and acquired with a FACSCanto II (BD, Franklin Lakes, NJ, USA) using TruCountTM tubes (BD, Franklin Lakes, NJ, USA) to determine the absolute number of CellTrace+ CD3+ cells in the samples as indicated by Solito et al. [168]. Finally, data were analyzed using FlowJo software (Treestar Inc.).

2.5 Statistical and Bioinformatics Analysis

Data obtained from flow cytometry regarding whole blood immunophenotyping underwent cluster analysis and t-distributed stochastic neighbor embedding (t-SNE). After discriminating doublets and excluding debris based on light scatter characteristics, cell events from each sample were saved in Flow Cytometry Standard (FCS) files and imported into the R/Bioconductor platform using the "flowCore" package. Each matrix was subsampled to 5x10^3 events per sample for a more precise calculation, then individually compensated and transformed using the Logicle transformation [169]. Subsequently, all samples at each time point were concatenated into a single matrix for both P and NP patients. FlowSOM metaclustering and t-SNE were performed on each matrix using the CATALYST package with default parameters. Cell type categorization was carried out considering specific parameters (FSC-A, SSC-A, HLA-DR, CD45, CD3, CD4, CD14, CD16). The quantities of different cell populations were reported as percentages of the total cell count using pie charts. Survival analyses

were performed using the "kmTCGA" and "survminer" packages. The Logrank test was used to compare survival curves, considering a p-value <0.05 as statistically significant. Figures were generated using R packages "CATALYST," "ggpubr," "flowCore," and "ggplot2." Mann-Whitney and Student's t-tests (paired and unpaired) were used to independently and comparatively analyze data obtained from P and NP patients. The Pearson correlation coefficient was used to measure the statistical relationship between c-FLIP expression in circulating CD14+ cells and their immunosuppressive potential.

2.6 Data searches and eligibility criteria

Additionally, a comprehensive search was conducted on April 1st from the following electronic databases: PubMed/MEDLINE (National Library of Medicine) and Scopus. A hand-searched reference list of the eligible articles and other overviews was also performed. Relevant keywords such as “IL-8”, “IL-8”, “interleukin8”, “interleukin-8”, “CXCL-8”, “CXCL8”, “NSCLC,” “nsqNSCLC,” “sqNSCLC,” “SCLC,” “lung,” “carcinoma,” “cancer,” “tumor,” "neoplasm," “small,” were used in varying combinations and connected with the Boolean operators. Preferred Reporting Items for Systematic Reviews and Meta-Analysis (PRISMA) statement was followed to report findings [170].

Studies’ inclusion criteria were: i) original article; ii) availability of English full-text; iii) IL-8 expression evaluations, including serum, plasma, tissue, and pleural effusion; iv) availability of hazard ratio (HR) and 95% confidence intervals (CI) for overall survival (OS), progression-free survival (PFS) and disease-free survival (DFS) or adequate data for their estimation. Investigations were excluded if they were: i) animal studies or essential research papers; ii) studies on gene polymorphisms; iii) studies containing histotypes different from lung cancer; iv) studies containing IL-8 expression evaluation reported as a continuous variable.

2.7 Study selection and data extraction

A two-step process drove the study selection. Initially, two independent authors examined potential eligible literature for title and abstract. Secondly, the two authors reviewed the remaining studies' eligibility for full text. Disagreements or uncertainties were resolved in discussion with a third reviewer. The following relevant information was extracted from each included study by two authors: i) name of the first author, ii) year of publication, iii) study design, iv) study sample size; v) number of patients with IL-8 evaluation available; vi) detection method; vii) IL-8 cut-off; viii) lung cancer histology; ix) tumor stage; x) type of treatment; xi) HR and 95% CI for OS; xii) HR and 95% CI for PFS; xiii) HR and 95% CI for DFS.

2.8 Assessment for risk of bias

The quality of each included study was assessed using the Newcastle-Ottawa Scale (NOS). The NOS scale evaluates the risk of bias through eight items assessing selection, comparability, and outcomes. The total score ranges from zero (high risk of bias) to nine (low risk of bias), and a final score of more than 6 points was classified as a high-quality study.

2.9 Data analysis

Data were cumulated by adopting a fixed and random-effect model according to the DerSimonian and Laird method [171]. Two subgroup analyses for OS, according to the method of IL-8 detection and type of therapy, were performed to assess the difference between plasma and tissue/pleural effusion detection and chemotherapy (CT) and ICIs and surgery and other treatments, including tyrosine kinase inhibitors (TKIs) or multiple therapies. Another subgroup analysis for PFS, according to the type of therapy, was performed to assess the difference between CT and ICIs and other treatments, including TKIs or multiple therapies. The prevalence of patients with overexpressed IL-8 was calculated for each study and considered for a meta-regression analysis. Publication bias was assessed through a funnel plot. Heterogeneity was analyzed using Cochran's Q test and quantified by

the I2 statistics: values lower than 25% and 50% were considered as low and moderate heterogeneity, respectively, while values up to 50% were considered as high heterogeneity. A leave-one-out influence analysis was performed to identify the contribution of each study to the overall effect. All analyses were performed using meta and metafor packages developed in R v.4.2.2.

2.10 Survival analysis on RNA-seq data

RNA-seq data and clinical information of patients with lung adenocarcinoma (LUAD) and lung squamous cell carcinoma (LUSC) were obtained from The Cancer Genome Atlas (TCGA) using the R package "curatedTCGAData" [172]. After selecting only primary tumor samples, the upper quartile normalized expression values (RSEM TPM) of IL8 were downloaded, and the log2(IL8 + 1) was used for the analysis. Prior to survival analysis, cut points for stratifying patients who express high or low levels of the IL8 gene were estimated in each dataset (LUAD, LUSC, and combination of the two) using the maximally selected rank statistics implemented in the R package "maxstat" (https://CRAN.R-project.org/package=maxstat). Kaplan-Meier curves were plotted using the R packages "RTCGA" (https://www.bioconductor.org/packages/release/bioc/html/RTCGA.html) and "survminer" (https://CRAN.R-project.org/package=survminer). P-values were calculated using the log-rank test, considering $p < 0.05$ statistically significant.

3. RESULTS

3.1 Results of the prospective study

3.1.1 Patients' characteristics and response to ICIs

In the prospective study of this thesis, 34 patients with advanced NSCLC treated with ICIs in different lines were included for the final analysis. Clinical and pathological characteristics are reported in **Table 1**.

Table 1. Patients' characteristics enrolled in the prospective study.

Characteristics	**Patients** **N = 34 (%)**	**NP** **N = 16 (%)**	**P** **N = 18 (%)**
Gender			
Male	23 (67.6)	12 (75.0)	11 (61.1)
Female	11 (32.4)	4 (25.0)	7 (38.9)
Age years, median (range)	72 (44-84)	72.5 (58-82)	72 (44-84)
ECOG performance status			
0	14 (41.2)	8 (50.0)	6 (33.3)
1	17 (50.0)	7 (43.8)	10 (55.6)
2	3 (8.8)	1 (6.2)	2 (11.1)
Smoker			
Never	7 (20.6)	1 (6.2)	6 (33.3)
Former	20 (58.8)	11 (68.8)	9 (50.0)
Current	7 (20.6)	4 (25)	3 (16.7)
Histology			
Adenocarcinoma	25 (73.5)	11 (68.8)	14 (77.8)
Squamous Carcinoma	9 (26.5)	5 (31.3)	4 (22.2)
EGFR Status			
Mutated	1 (2.9)	0 (0.0)	1 (5.6)
Wild Type	33 (97.1)	16 (100.0)	17 (94.4)
PDL1 percentage			
<1%	3 (8.8)	1 (6.2)	2 (11.1)
≥1%-<50%	15 (44.1)	5 (31.3)	10 (55.6)
≥50%	16 (47.1)	10 (62.5)	6 (33.3)
Immunotherapy Agent			
Pembrolizumab	16 (47.1)	10 (62.5)	6 (33.3)
Nivolumab	14 (41.2)	4 (25.0)	10 (55.6)
Atezolizumab	4 (11.7)	2 (12.5)	2 (11.1)

Line of immunotherapy			
First	16 (47.1)	10 (62.5)	6 (33.3)
Second	18 (52.9)	6 (37.5)	12 (66.7)

Figure 1 displays the responses to immunotherapy per patient based on the maximum percentage reduction of the target lesion according to RECIST criteria.

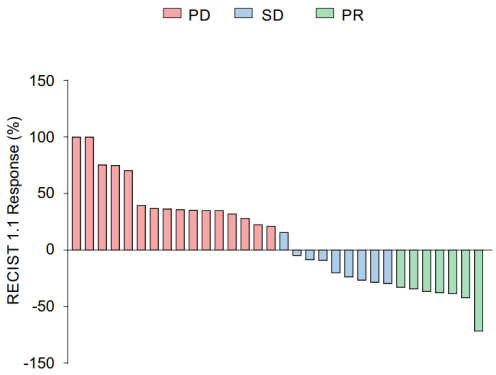

Figure 1. Waterfall plot of the study population's responses to immunotherapeutic treatment, based on the maximum percentage reduction in the tumor and the corresponding classification according to RECIST criteria (Response Evaluation Criteria in Solid Tumors). Two patients were deemed non-evaluable.
Abbreviations: PD: progressive disease, SD: stable disease, PR: partial response.

3.1.2 ICI immunotherapy affects the blood immune landscape in non-progressor NSCLC patients

As expected, P patients had a significantly lower survival probability compared to NP patients (**Figure 2**). Several studies have reported that the lung immune prognostic index (LIPI) score is one of the most promising and reliable tools for predicting ICI resistance in lung cancer patients [99]. In agreement with these premises, NSCLC patients enrolled in this study with either “good” (0, green line) or “intermediate” (1, yellow line) LIPI score showed a significantly higher survival probability compared to patients identified with a “poor” LIPI score (2, purple line) at baseline (T0), regardless of whether they belonged to the P or NP group of patients (Figure 1b). All four patients showing the highest LIPI scores

(purple line) were included in the P patient sub-group at T1, suggesting that they did not respond to ICI immunotherapy. Collectively, these results confirmed LIPI as a predictive score for ICI treatment in patients with NSCLC (**Figure 3**).

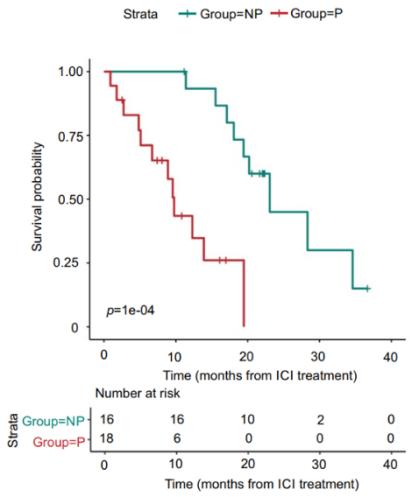

Figure 2. Kaplan-Meier curves representing overall survival (calculated from the start date of ICI treatment) of patients with NSCLC (n=34), stratified based on clinical response into non-progressors (NP, green) and progressors (P, red).

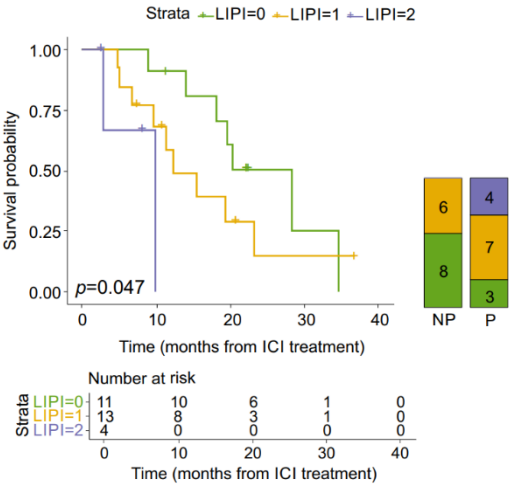

Figure 3. Kaplan – Meier curves (left) reporting the overall survival (OS, calculated from the date of start of ICI-treatment) of NSCLC patients (n = 28) stratified by lung immune prognostic index (LIPI) score at baseline as good (0, green), intermediate (1, yellow) and poor (2, purple). The overall log-rank test p = .0047. Bonferroni corrected LIPI 1 vs. LIPI 0 p = 0.48, LIPI 1 vs LIPI 2 p = 0.72, LIPI 0 vs LIPI 2 p = .0147). Graph bar (right)

reported NSCLC patient's fractions with 0 (green), 1 (yellow), or 2 (purple) LIPI score in non-progressor (NP) and progressor (P) NSCLC patients (n = 28). The p-value (log-rank test) was calculated to test differences among the three groups.

The LIPI score considers the neutrophil/leukocytes (NLR) ratio and lactate dehydrogenase (LDH) plasma levels. A deeper analysis of circulating immune soluble factors and cell subsets could provide additional candidates for predicting ICI efficacy in NSCLC patients. Indeed, neutrophils were significantly higher in patients showing a "poor" LIPI score (**Figure 4**); among lymphocyte subsets, only natural killer (NK) cell count significantly diverged in this patient subgroup compared to patients characterized with either a "good" or an "intermediate" LIPI score (**Figure 4**). In addition to the LIPI score, we also assessed other potential parameters, such as NLR, neutrophil-to-T lymphocytes (NTR), platelets-to-lymphocytes (PLR), neutrophils-to- CD4+ T cells, monocytes-to-lymphocytes (MLR), and monocyte-to-T lymphocyte (MTR) ratios; however, none of them at baseline were able to predict ICI response. Nevertheless, we detected a significant reduction in some of these parameters only in NP patients as a possible consequence of immunotherapy response, thus indicating the ability of PD-1/PD-L1 blockade not only to influence T cell effectiveness but also to alleviate systemic inflammation.

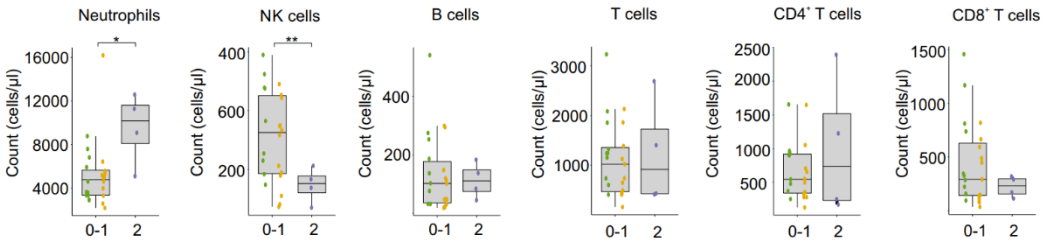

Figure 4. Box plots showing, at baseline, circulating neutrophils, NK cells, B cells, T cells, CD4+, and CD8+ T cells count in NSCLC patients (n = 28), classified by LIPI score (0 green, one yellow, two purple). Mann-Whitney or Student's t-test. *p < .05, **p < .01.

To further investigate ICI treatment's effects, we quantified different pro-inflammatory cytokines in plasma samples before (T0) and after (T1) ICI

immunotherapy. In the timeframe from T0 to T1, PD-1/PD-L1 inhibition significantly restrained the plasma levels of IL-6, IL-8, C–C chemokine ligand 4, IL-7, and IL-1β in NP patients associating ICI responsiveness to a contraction in systemic inflammation (**Figure 5**). Other inflammation-associated cytokines, such as IL-8 and IL-1β, increased in P patients over time. Their plasma levels at T1 were higher than those detected in NP patients (**Figure 5**). Interestingly, IL-2 remained higher in NP patients at both observational time points (**Figure 5**). Collectively, only in NP patients does ICI-based immunotherapy promote the time-dependent mitigation of several pro-inflammatory mediators whose basal levels were not predictive of response to immunotherapy.

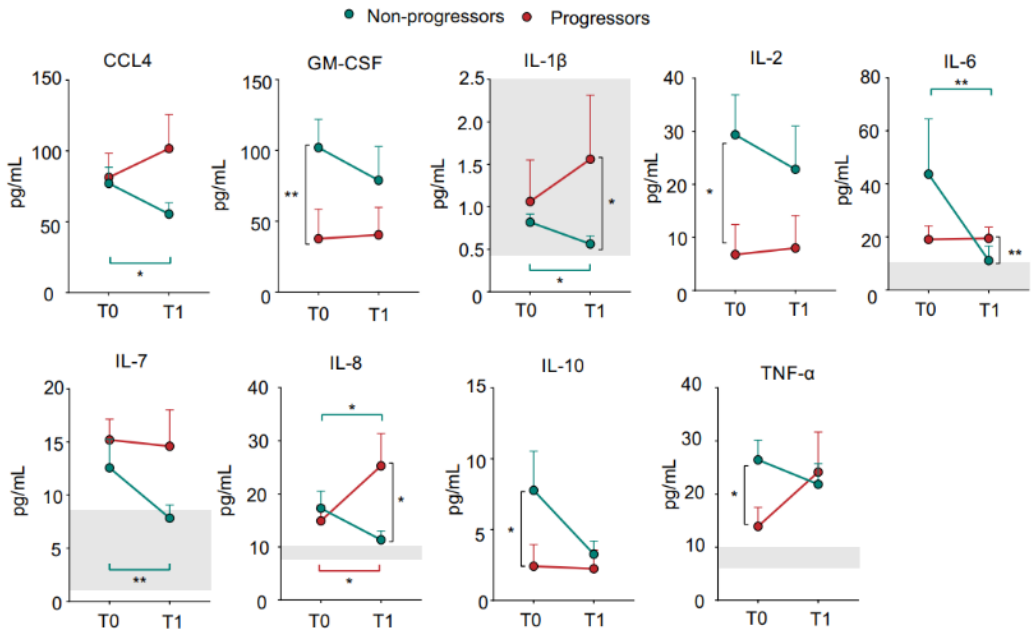

Figure 5. Effect of ICI immunotherapy on inflammation-associated cytokines in NSCLC patients. (a) CCL4. GM-CSF, IL-1β, IL-2, IL-6, IL-7, IL-8, IL-10, and TNF-α levels in plasma samples isolated from progressor (red) and non-progressor (green) NSCLC patients before (T0) and after (T1) ICI treatment (n = 34). The reference range of healthy subjects is reported with the light gray boxes. The data are shown as the mean ± SEM. Mann-Whitney and Wilcoxon test *p <.05, **p <.01. Stars and lines related to statistical analyses are indicated in red for comparison between T0 and T1 in Progressor (P) patients; green for comparison between T0 and T1 in Non-Progressor (NP) patients; black for comparison between P and NP patients at either T0 (left) or T1 (right), respectively.

We then assessed the impact of ICI therapy on circulating immune cell populations. T-distributed stochastic neighbor embedding (t-SNE) and clustering analysis of peripheral blood revealed an increased proportion of T (from 13% to 16%), B (from 1% to 3%), and NK (from 4% to 5%) lymphocytes, with a concomitant decrease in neutrophils (from 68% to 62%) in NP patients after ICI treatment (**Figure 6**). This unbiased analysis showed no clear alteration of circulating populations in P patients, except for a weak increase in monocytes (from 9% to 10%) (**Figure 6**). Flow cytometry analysis confirmed an ICI-dependent increase in lymphocyte count in NP patients (**Figure 7**). NK cells were higher in NP patients than in P patients, both before and after ICI treatment (**Figure 7**). Similarly, CD8+CD4+ T cells increased only in the NP patient subgroup after ICI immunotherapy. Conversely, monocyte count significantly discriminated NP and P patients at the baseline (**Figure 7**). To evaluate whether PD-1/PD-L1 inhibition could influence the monocyte compartment, we assessed the levels of three major monocyte populations: classic (CM, CD14+CD16− cells), non-classic (NCM, CD14dimCD16+ cells), and intermediate (IM, CD14+CD16+ cells) monocytes. Only the NCM count was significantly higher in NP patients than in P patients at T1. In contrast, an increasing trend was detected for the other two monocytic subsets in NP patients at T0. These data indicate that ICI therapy can reprogram systemic immunity by increasing lymphocyte frequency and altering myeloid cell composition.

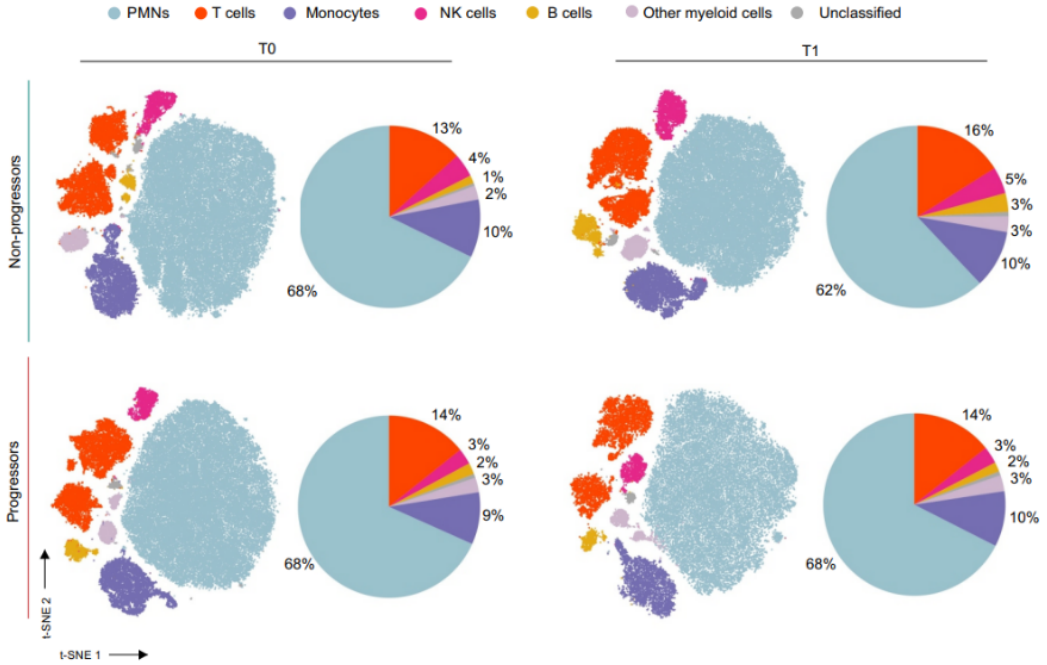

Figure 6. Effect of ICI immunotherapy on circulating immunological profile in NSCLC patients. T-distributed stochastic neighbor embedding (t-SNE) analysis on flow cytometry events following debris and doublet exclusion in non-progressor (NP) and progressor (P) patients before (T0) and after (T1) ICI treatment (T0-P and NPn = 15, T1-P n = 9, T1-NPn = 15). Pie charts representing cell population proportions derived from clustering and t-SNE analysis for each group and time point.

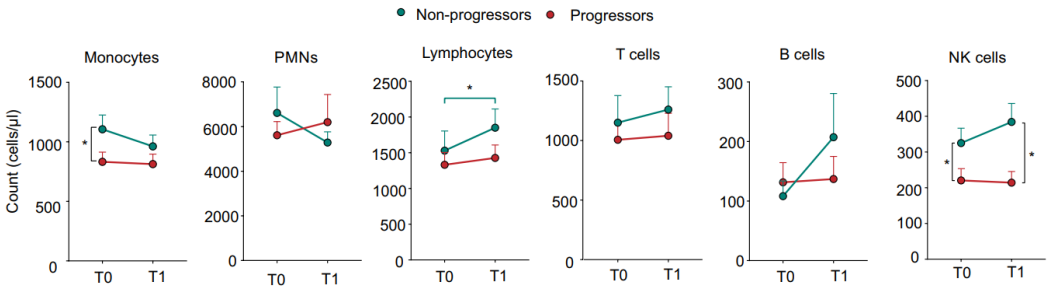

Figure 7. Effect of ICI immunotherapy on circulating immunological profile in NSCLC patients. Monocytes, PMNs, lymphocytes, T, B, and NK cell count in progressor (P, red) and non-progressor (NP, green) NSCLC patients before (T0) and after (T1) ICI treatment (n = 34). Mann– Whitney test. The data are shown as the mean ± SEM. *p < .05. Stars and lines related to statistical analyses are indicated in red for comparison between T0 and T1 in Progressor (P) patients; green for comparison between T0 and T1 in Non-

Progressor (NP) patients; black for comparison between P and NP patients at either T0 (left) or T1 (right), respectively.

3.1.3 ICI immunotherapy modifies immune-suppressive features of circulating M-MDSCs

One of the critical inducers of primary and secondary resistance to ICI therapy is the accumulation of several unconventional myeloid cell subsets with pro-tumoral functions defined by MDSCs [173]. Therefore, we assessed the ability of PD-1/PD-L1 inhibition to affect the immunosuppressive functions of M-MDSCs identified as FLIP-overexpressing CD14+ cells. At baseline, NSCLC-derived CD14+ cells showed higher c-FLIP expression than healthy donors (HDs) (**Figure 8A**), which is in agreement with previous reports on PDAC patients [157]. To further investigate FLIP in myeloid cells, we performed a t-SNE analysis of flow cytometry data from both P and NP patients, revealing a higher expression of c-FLIP in CD14+CD16−HLA-DRlow cells that resemble a conventional subgroup of M-MDSCs. We defined that c-FLIP mediates the acquisition of immunosuppressive features in monocytes [157]. Accordingly, we observed a direct correlation between c-FLIP expression in CD14+ cells isolated from patients before ICI treatment and their ability to suppress the in vitro proliferation of activated CD3+ T lymphocytes (**Figure 8B**). FLIP expression in circulating M-MDSCs at T0 was similar in both P and NP patients. In contrast, after ICI treatment, a substantial reduction in FLIP expression was detected only in the NP patient cohort (**Figure 8C**). However, this reduction did not involve specific conventional monocyte subsets. Furthermore, monocytes isolated from NP patients partially lost their ability to inhibit T-cell proliferation (**Figure 8D**). Notably, in vitro, immuno-suppressive activity was tested simultaneously by co-culturing thawed CD14+ cells isolated from patients at both T0 and T1 with the same in vitro activated allogeneic T cells isolated from buffy coat to standardize functional evaluation. Collectively, our data highlight that ICI therapy affects M-MDSC-dependent immunosuppressive activity, probably due to the decrease of c-FLIP expression.

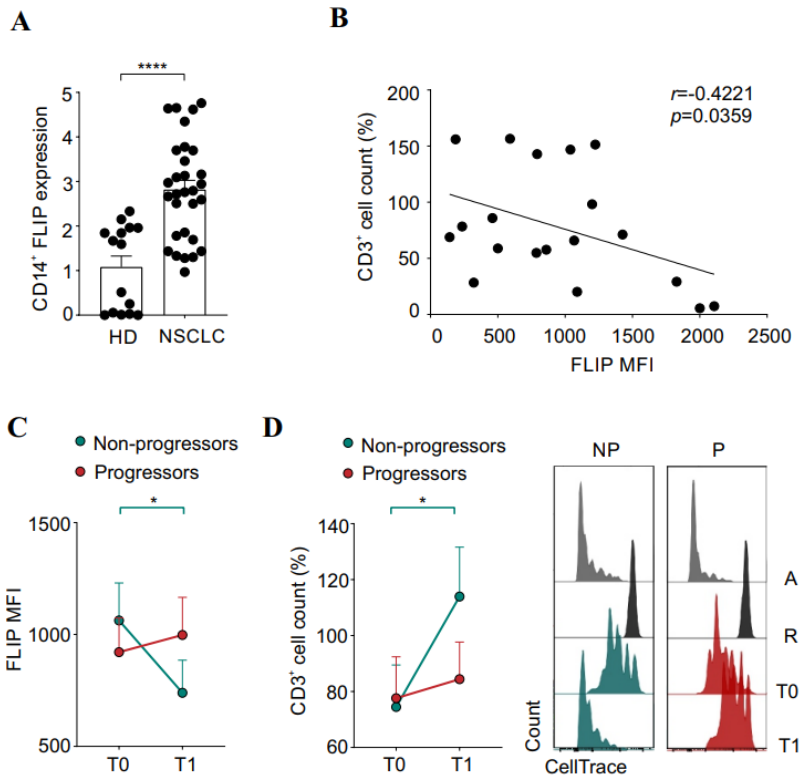

Figure 8. Effect of ICI immunotherapy on immunosuppressive features of M-MDSCs in NSCLC patients. (A) c-FLIP expression evaluated by FACS analysis and reported as mean fluorescence intensity (MFI), FMO (fluorescence minus one) corrected, in circulating CD14+ cells from healthy donors (HD) and NSCLC patients. Mann–Whitney test. (B) Circulating CD14+ cells isolated from NSCLC patients before ICI treatment were co-cultured with HD-derived, α-CD3, and α-CD28 activated PBMCs to evaluate their immunosuppressive ability. The percentage of CellTrace+CD3+ T lymphocyte cell count deriving from immunosuppression assays was correlated with CD14+ c-FLIP expression evaluated as FMO-corrected MFI. Pearson r correlation. (C) FMO corrected c-FLIP MFI of CD14+ cells in progressor (P, green) and non-progressor (NP, red) patients before (T0) and after (T1) ICI treatment (T0-P n = 16, T1-P n = 10, T0-NPn = 15, T1-NPn = 14). Mann-Whitney and Wilcoxon test. (D) Representative proliferation peaks of CellTrace+CD3+ T lymphocytes following the co-culture with circulating CD14+ cells isolated from progressor (red) and non-progressor (green) NSCLC patients before (T0) and after (T1) ICI treatment (left) (A: Activated control, R: resting control). Percentage of CellTrace+CD3+ T lymphocyte cell count following the co-culture with circulating CD14+ cells isolated from progressor (red) and non-progressor (green) NSCLC patients before (T0) and after (T1) ICI treatment (T0-P n = 8, T1-P n = 9, T0-NPn = 12, T1-NPn =

12) (right). All values are normalized on activated T cells in the absence of myeloid cells. Mann-Whitney and Wilcoxon test. The data are shown as the mean ± SEM.
*p < .05, ****p < .0001. Stars and lines related to statistical analyses are indicated in green or red if they referred to non-progressor or progressor patients, respectively.

3.2 Results of the metanalysis on IL-8 and lung cancer

3.2.1 Study selection

Among the 2,655 produced records, 741 duplicates were removed (**Figure 9**). A total of 1,819 investigations were excluded after title and abstract screening, and 13 studies were definitively included in the meta-analysis after full-text assessment. Of note, three studies were considered two different studies in the meta-analysis since two distinct cohorts of patients were reported [163,174,175].

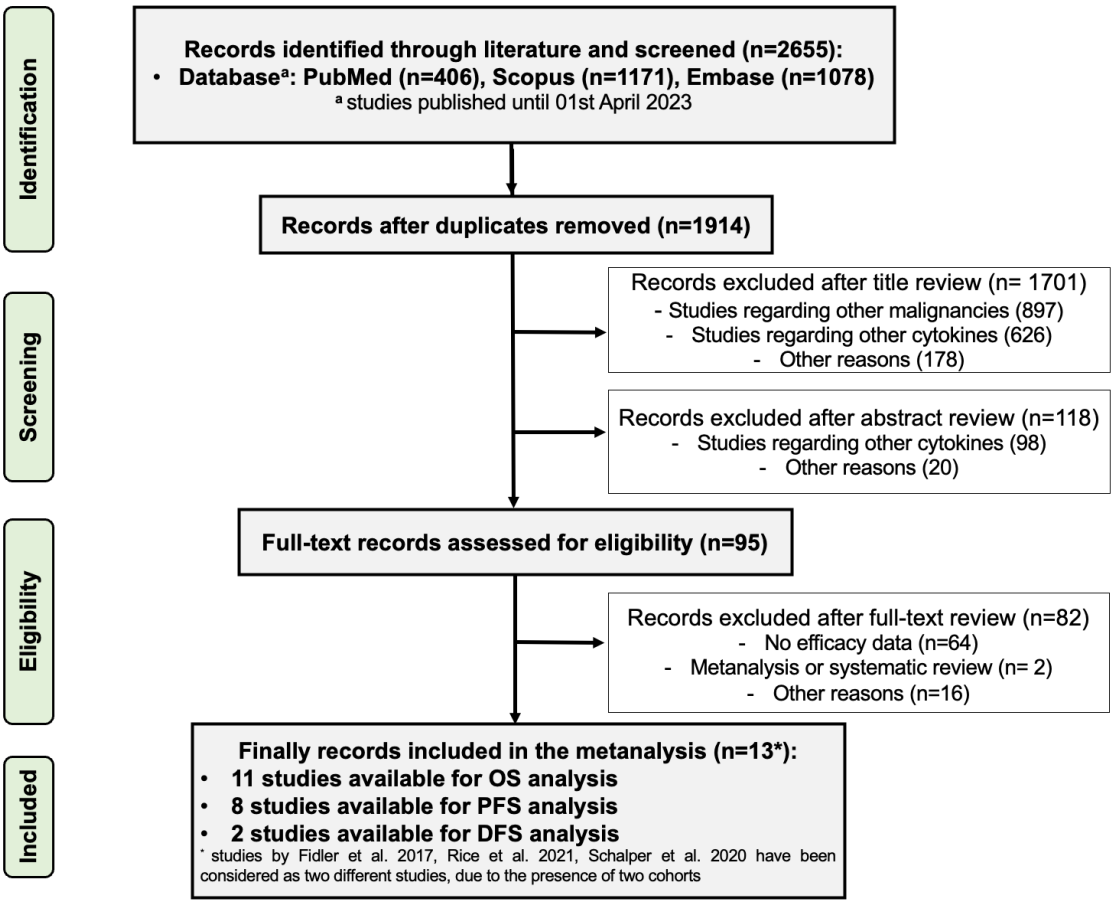

Figure 9. Flow diagram of the meta-analysis.

3.2.2 Study characteristics

In **Table 2**, we have summarized the characteristics of the included studies. In brief, seven studies utilized a prospective design [174-178], and overall, the included investigations were published from 2002 to 2021. Among the 2,113 patients with lung cancer (both NSCLC and small cell lung cancer - SCLC), the evaluation of IL-8 at baseline was conducted in 1,949. The IL-8 analysis was based on a plasma sample (10 out of 13) [163,174,175,177-180], tissue (2 out of 13) [181,182], or pleural effusion sample (1 out of 13) [176]. As shown in **Table 2**, different IL-8 cut-offs were used. Six studies prospectively evaluated the IL-8 levels in patients treated with chemotherapy [174-178], while five studies involved patients treated with immunotherapy [163,175,180]. The risk of bias assessment revealed that almost all the studies reached moderate/high quality (**Table 2**). **Table 3** summarizes the main results of the studies included in the meta-analysis. We identified eleven [174-177,179,181,182], eight [163,174,175,178,180], and two [176,181] eligible trials for OS, PFS, and DFS analysis, respectively.

Study	***Study design***	***Study sample (n)***	***IL8 data (n)***	***IL8 detection***	***IL8 cut-off***	***Histology***	***Stage***	***Therapy***	***NOS total score***
Cheng D, 2013	Prospective	71	71	Pleural effusion	1693 pg/ml	All, including SCLC	IV	CT	8
Fidler MJ, 2017 *Cohort 1*	Prospective	111	32	Plasma	10 vs 90th	NSCLC	IIIB-IV	CT	8
Fidler MJ, 2017 *Cohort 2*	Prospective	111	79	Plasma	10 vs 90th	NSCLC	IIIB-IV	Target therapy	8
Gu L, 2021	Retrospective	232	232	Tissue	IHC >3	NSCLC	I-IIIA	Surgery	8
Orditura M, 2002	Prospective	60	60	Plasma	79.5 pg/ml	NSCLC	III-IV	CT	6
Seike M,	Retrospective	80	30	Tissue	6.4	NSCLC	I	Surgery	7

2007					pg/mg				
Ryan BM, 2014	Retrospective	548	548	Plasma	75th	All, including SCLC	I-IV	NA	6
Rice SJ, 2021 *Cohort 1*	Prospective	235	184	Plasma	NA	NSCLC	NA	IO/CT/ target therapy	6
Rice SJ, 2021 *Cohort 2*	Prospective	235	51	Plasma	NA	SCLC	NA	IO/CT	6
Sui X, 2021	Prospective	31	31	Plasma	4.34 pg/ml	NSCLC	IIB-IIIB	CT/RT	8
Zhou J, 2021	Retrospective	156	42	Plasma	7 pg/ml	All, including SCLC	IV	IO	7
Schalper KA, 2020 *Cohort 1*	Retrospective	184	184	Plasma	23 pg/ml	Squamous NSCLC	IV	IO	8
Schalper KA, 2020 *Cohort 2*	Retrospective	405	405	Plasma	23 pg/ml	Non-squamous NSCLC	IV	IO	8

Table 2. Characteristics of the studies included in the meta-analysis.

Study	**HR OS (95% CI) *p-value***	**HR PFS (95% CI) *p-value***	**HR DFS (95% CI) *p-value***
Cheng D, 2013	2.84 (1.987-3.689) 0.001	NA	2.38 (1.245-3.555) 0.001
Fidler MJ, 2017 (*Cohort 1*)	5.11 (1.86-14.03) 0.002	4.94 (1.77-13.76) 0.002	NA
Fidler MJ, 2017 (*Cohort 2*)	1.18 (0.92-1.51) 0.205	0.92 (0.78-1.09) 0.339	NA
Gu L, 2021	1.27 (0.908-1.763)	NA	1.19 (0.882-1.602) 0.256

	0.164		
Orditura M, 2002	2.89 (1.40-5.97) 0.0025	NA	NA
Seike M, 2007	2.66 (1.04-6.82) 0.03	NA	NA
Ryan BM, 2014	1.23 (1.00-1.52) 0.047	NA	NA
Rice SJ, 2021 *(Cohort 1)*	1.3 (1.1-1.5) 0.004	1.2 (1.00-1.4) 0.019	NA
Rice SJ, 2021 *(Cohort 2)*	1.00 (0.88-1.2) 0.806	1.1 (0.92-1.2) 0.407	NA
Sui X, 2021	NA	0.79 (0.630-0.985) 0.036	NA
Zhou J, 2021	NA	0.32 (0.07-1.36) 0.087	NA
Schalper KA, 2020 *(Cohort 1)*	1.84 (1.19-2.83) 0.0051	1.28 (0.81-2.00)	NA
Schalper KA, 2020 *(Cohort 2)*	1.90 (1.42-2.53) <0.0001	1.60 (1.19-2.15)	NA

Table 3. Results of the studies included in the meta-analysis.

3.2.3 The overall prognostic impact of IL-8

The eleven studies included in the OS analysis revealed that patients with high levels of IL-8 have a higher chance of shorter OS compared to patients with normal levels of IL-8 (HR = 1.65 95% CI 1.29-2.11, heterogeneity I2 = 83%; $p < 0.001$) (**Figure 10**). A random effect model was used to calculate the effect size

since the included studies showed a high heterogeneity (I = 83%, p < 0.001). Through the funnel plot and the Egger's test (p = 0.013), we could assess the presence of asymmetry and, therefore, the presence of publication bias.

We observed that six studies have standard errors larger than expected, leading to possible outliers. The leave-one-out validation [183] suggested that the study by Rice S.J. and colleagues, 2021 (cohort 2) [175] is particularly influent on the effect size, while the study by Cheng D. et al., 2013 [176] is influent on both heterogeneity and effect size. The simple outlier removal algorithm applied to the random-effects meta-analysis was detected as an outlier in the study by Rice S.J. et al., 2021 (cohort 2) [175]. Nevertheless, after its removal, the results appeared similar, giving robustness to our previous findings (HR = 1.75 95% CI 1.36-2.24).

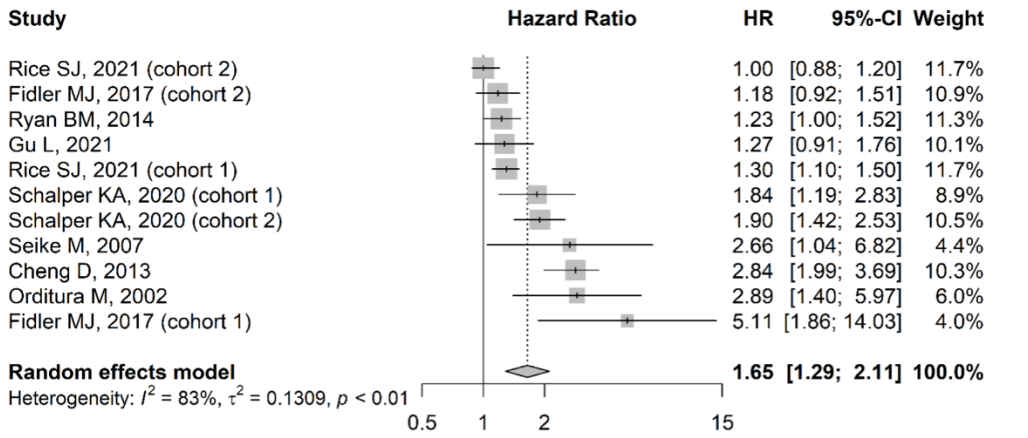

Figure 10. Forest plot of hazard ratios (HR) comparing OS in patients with normal and high levels of IL-8. HR for each trial is represented by the squares, and the horizontal line crossing the squares represents the 95% confidence interval (CI). The diamond represents the estimated overall effect based on the meta-analysis random effects of the trials. All statistical tests were two sides.

The eight studies included in the PFS analysis revealed no significant differences between patients with high and normal levels of IL-8 (HR = 1.14 95% CI 0.90-1.44, heterogeneity I2 = 78%; p < 0.001) (**Figure 11**). A random effect model was used to calculate the effect size since the included studies showed a high heterogeneity (I = 78%, p < 0.001). The funnel plot shows slight asymmetry and, therefore, no presence of publication bias. Egger's test was not performed since it may lack the statistical power to detect bias when the number of studies is small

(less than ten). We observed that two studies have a larger standard error than expected. To perform further analysis, the leave-one-out validation suggested that the study by Fidler M.J. et al., 2017 (cohort 1) [174] is particularly influent on heterogeneity, and the study by Sui X. et al., 2021 [178] is influent on both heterogeneity and effect size. Applying a simple outlier removal algorithm to our meta-analysis, the study by Fidler M.J. et al., 2017 (cohort 1) [174] was detected as an outlier. Nevertheless, after removing this outlier, the study results appear similar (HR = 1.07 95% CI 0.89-1.30).

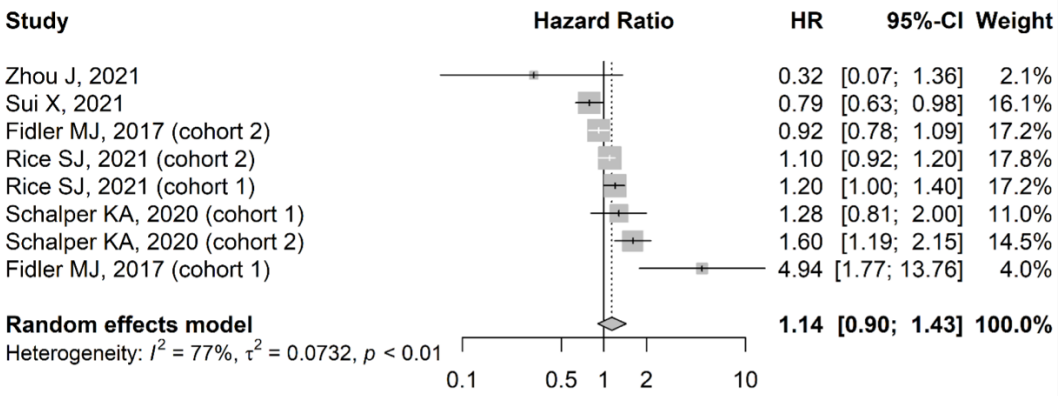

Figure 11. Forest plot of hazard ratios (HR) comparing PFS in patients with normal and high levels of IL-8. HR for each trial is represented by the squares, and the horizontal line crossing the squares represents the 95% confidence interval (CI). The diamond represents the estimated overall effect based on the meta-analysis random effects of the trials. All statistical tests were two sides.

Among the eleven studies in our research, just two included results about DFS—more than these numbers are required to perform a robust meta-analysis. However, combining these two studies, no significant difference between patients with high and normal levels of IL-8 had been shown (HR = 1.63 95% CI 0.83-3.19, heterogeneity I2 = 80%; p = 0.03) (**Figure 12**). A random effect model was used to calculate the effect size since the included studies showed a high heterogeneity (I = 78%, p < 0.001). No further analyses were performed, considering the exiguous number of studies.

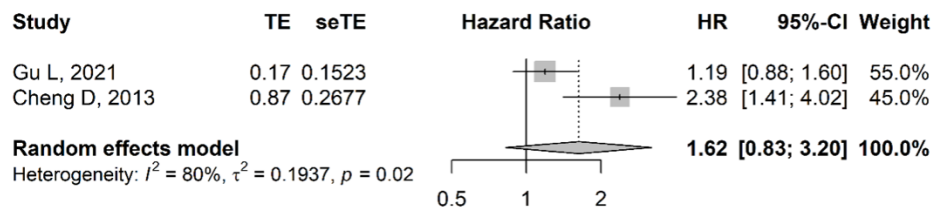

Figure 12. Forest plot of hazard ratios (HR) comparing DFS in patients with normal and high levels of IL-8. HR for each trial is represented by the squares, and the horizontal line crossing the squares represents the 95% confidence interval (CI). The diamond represents the estimated overall effect based on the meta-analysis random effects of the trials. All statistical tests were two sides.

3.2.4 Subgroup analysis

A subgroup analysis suggested a higher chance of shorter OS, irrespective of the type of IL-8 detection method (plasma/tissue/pleural effusion). This analysis included nine studies (eight studies with plasma detection and three studies with tissue/pleural effusion detection) that showed high heterogeneity in each subgroup (plasma: I2=78%, p < 0.01; tissue/pleural effusion: I2=84%, p < 0.01), therefore random effects model was performed to summarize the hazard ratios for both detections (HR plasma = 1.50 95% CI 1.17-1.93; HR tissue/pleural effusion = 2.04 95% CI 1.14-3.63). No significant difference was detected between patients subjected to plasma and tissue/pleural effusion detection (p=0.34) (*Figure A1-Appendix*).

Another subgroup analysis regarding treatment types [CT vs. ICIs vs surgery vs other (including TKIs and multiple treatments)] was performed for both OS and PFS. The PFS analysis included eight studies (one study with CT, three studies with ICIs and four studies with other therapies) that showed high heterogeneity (I2 = 77%, p < 0.01) and moderate-high heterogeneity in each subgroup (ICIs: I2 = 74%, p < 0.01; CT: I2 = 57%, p < 0.10), therefore random effects model was performed to summarize the hazard ratios for all therapies (HR CT = 4.94 95% CI 1.77-13.77; HR ICIs = 1.39 95% CI 1.03-1.88; HR other = 1.00 95% CI 0.84-1.19) (*Figure A2-Appendix*); whereas OS analyses included ten studies (three

studies with CT, two studies with surgery, two studies with ICIs and three with other therapies) showed a moderate heterogeneity (I2 = 85%, $p < 0.01$), therefore we decided to perform a random effects model to summarize the hazard ratios of all subgroup, even if each subgroup showed low/moderate heterogeneity (HR CT = 2.97 95% CI 2.26-3.91; HR surgery = 1.60 95% CI 0.81-3.15; HR ICIs = 1.88 95% CI 1.48-2.39, HR other = 1.15 95% CI 0.97-1.36) (*Figure A3-Appendix*). A significant difference was detected between patients treated with CT, ICIs, surgery, and other therapies in both PFS ($p < 0.01$) and OS ($p < 0.01$).

3.2.5 Survival data obtained from The Cancer Genome Atlas (TCGA)

To further evaluate the prognostic value of IL8 gene expression on lung cancer, we performed an OS analysis using RNA-seq data from The Cancer Genome Atlas (TCGA). After combining the normalized gene expression data of lung adenocarcinoma (LUAD, n=502) and lung squamous cell carcinoma (LUSC, n=494), we plotted Kaplan-Meier curves stratifying the patients for IL8 expression (see methods section). We observed that patients with higher IL8 expression had a generally lower OS than those with lower expression (**Figure 13**). A similar trend was observed individually on LUAD and LUSC datasets (*Figure A4/A5-Appendix*).

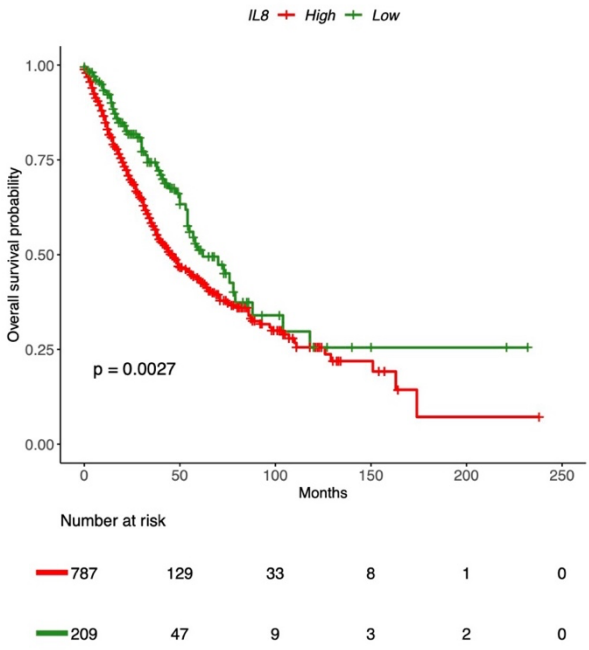

Figure 13. Kaplan-Meier curve showing the overall survival probability of lung cancer patients of the TCGA dataset (LUAD and LUSC combined) stratified for IL8 high and low expression (see methods section).

4. DISCUSSION

Considering the overall impact of immunotherapy in lung cancer treatment, there is an urgent need to evaluate and, possibly, validate predictive and prognostic biomarkers in the light of tailored oncology. Despite advances in treatment modalities, the five-year survival rate for patients with lung cancer remains low [184]. The introduction of targeted therapies and ICIs has consistently improved lung cancer patients' survival. However, after an undefined period, disease progression and treatment resistance, caused by both cancer cell-intrinsic factors and mechanisms within the tumor microenvironment, inevitably occur [185,186]. Therefore, it is crucial to understand the mechanisms underlying cancer progression and identify potential prognostic and predictive factors that can guide treatment choices.

In this light, the prospective section of this thesis evaluates the effects of ICI therapy on modulating MDSC-associated immunosuppression and inflammation. Our findings indicate that immunotherapy treatment exclusively leads to a

contraction of circulating factors such as CCL4, IL-1β, IL-6, IL- 7, and IL-8 in the NP. All these soluble factors were identified as potential targets to improve immunotherapy effectiveness [187-190], highlighting how the repression of these pro-inflammatory cytokines is essential to trigger a successful anti-tumor immune response. In particular, IL-8 appears to play a critical role in defining ICI effectiveness in our patient cohort since, in the time window between T0 and T1, it was significantly decreased in the plasma of NP patients while significantly deepening in P patients. On the other hand, high levels of GM- CSF, IL-2, IL-10, and TNFα before ICI treatment could define NP patients and may serve as potential predictive biomarkers for response to immunotherapy. Indeed, it is mandatory to validate all these parameters using independent and large patient cohorts and test these parameters in different cancers. Despite the limited number of patients tested in this work, our findings revealed that P patients never showed ICI-dependent alterations in tested circulating factors, except for IL-8, suggesting that, probably, these patients are immune and unresponsive. A deeper analysis of the cell source of these inflammation-associated mediators is worthy of future studies to develop innovative therapeutic approaches and more efficient tools for early diagnosis of resistance to therapy.

The Immunology Department of the University of Verona previously reported that c-FLIP-expressing myeloid cells released several inflammation-associated molecules such as IL-6 and TNF-α by a “steered” NF-κB activation, which also resulted in enhanced STAT3-signaling activation [157,191]. Furthermore, c-FLIP promotes the acquisition of immunosuppression-associated features that can explain the inhibition of T cell activation and proliferation, i.e., receptor–ligand interactions (i.e., PD-L1 axis), metabolic pathways (i.e., IDO1-dependent tryptophan metabolism pathway), and production of cytokines (i.e., IL-6) [157]. Thus, we exploited c-FLIP detection to monitor changes in MDSCs by immunotherapy. In line with previous findings in PDAC [157] and COVID-19 [158] patients, we found a high level of c-FLIP expression in NSCLC patient-derived monocytes before immunotherapy treatment. Moreover, the immunosuppressive functions of monocytes isolated from patients with NSCLC directly correlated with the expression of c-FLIP. It is important to highlight that

c-FLIP expression by t-SNE analysis was preferentially restricted to a classical monocyte subset characterized as CD14+HLA-DR low cells, which identify a specific MDSC sub-group (also defined as MDSC4), which can discriminate PDAC patients with metastatic disease [192]. ICI treatment potentially reduced c-FLIP expression in circulating monocytes and their inhibitory properties only in NP patients. Coupled with FLIP expression of this pro-tumor cell subset, NP patients showed a significant increase in circulating lymphocytes, especially NK cells and CD8+CD4+ T cells. Recently, an enrichment in CD4+CD8+ T cells among patients who ultimately responded to ICI has been reported [193]. Notably, double-positive T cells were characterized by potent tumor major histocompatibility complex (MHC)-dependent reactivity, suggesting a critical role of these cells in specific ICI-induced effector lymphocytes [193].

As above-mentioned, despite reproducible positive results, only a minority (<20%) of the patients show long-term benefit from ICI immunotherapy, and most will progress at any time during treatment; furthermore, a non-negligible proportion of patients receiving ICI do not respond to treatment despite high PD-L1 expression. Current biomarkers for predicting the response to ICI therapy are usually based on biopsies from solid tumors, including the PD-L1 status. These biomarkers require invasive techniques that pose significant challenges that can be overcome using liquid biopsies to analyze circulating immune parameters. Our study suggests new potential and more advantageous targets, including monocyte and NK count and inflammation-associated soluble mediators such as TNF-α, GM-CSF, IL-2, and IL-8. Furthermore, we described a rapid variation of additional immunological features following immunotherapy only in NP patients, including c-FLIP expression in monocytes, CD4+CD8+ T and NK lymphocyte counts, and inflammatory cytokines, such as IL-6. Recently, blood-based proteomic screening revealed a predictive signature able to stratify NP and P patients, in which IL-6, neutrophil-related proteins, Janus kinase-STAT, and NF-κB signaling path-ways were identified as key players in promoting resistance to ICI [194].

Based on the prospective part of this study, to potentially validate the prognostic role of a circulating biomarker, in particular IL-8, we performed a meta-analysis

that revealed that patients with a high level of IL-8 had a higher likelihood of experiencing a shorter OS when compared to patients with a normal level of IL-8 at the moment of diagnosis (HR = 1.65 95% CI 1.29-2.11, $p < 0.001$). This finding was consistent with data previously collected in other meta-analyses involving several solid cancers [165,195]. Interestingly, Mao et al. reported that baseline IL-8 high levels were significantly associated with poorer OS in patients treated with ICIs (HR = 1.88 95% CI 1.70-2.07, $p < 0.00001$) [195].

Subgroup analyses were conducted to examine the impact of different factors on patients' outcomes. One subgroup analysis explored the type of IL-8 detection method performed in the studies, specifically comparing plasma detection with detection in tissue or pleural effusion samples. Based on nine studies, this analysis indicated that regardless of the method used to measure IL-8 levels, an elevated level of IL-8 was consistently associated with poorer OS outcomes. These specific results underline that IL-8 analysis may be easily assessed and monitored with a blood test.

Another subgroup analysis focused on the impact of different treatment modalities on PFS and OS. The treatments considered in this analysis included CT, IO, TKIs, and surgery. The results demonstrated a significant difference in both PFS ($p < 0.01$) and OS ($p < 0.01$) among patients treated with CT, IO, and surgery when compared with other treatments (including TKIs). This differential impact of IL-8 on the predictive value of immunotherapy versus TKIs may be attributed to the underlying mechanisms of action associated with these treatment modalities. In particular, high levels of IL-8 may have detrimental effects on inflamed tumors, which are typically responsive to ICIs [196]. Prior analyses demonstrated an association between increased circulating immunosuppressive myeloid-derived suppressor cells (MDSCs) and high levels of IL-8 in the plasma [197,198]. In addition, transcriptomic analysis of IL-8-producing myeloid cells supports their role in hindering adaptive immunity through upregulation of myeloid proinflammatory genes and downregulation of genes involved in antigen presentation and interferon response, which are linked to the response to ICIs [164,199].

Regarding PFS analysis, no significant differences between patients with high and normal levels of IL-8 (HR = 1.14 95% CI 0.90-1.44, p < 0.001) were detected. Conversely, the two meta-analyses available regarding the role of IL-8 in cancer survival demonstrated a significantly shorter OS in patients with high levels of IL-8 and a significantly reduced PFS across several tumor histologies [165,195].

On the other hand, only two studies out of 11 provided data on DFS. These numbers are inadequate for a reliable meta-analysis. Nevertheless, when these two studies were combined, no significant difference was observed between patients with high and normal IL-8 levels. To the best of our knowledge, no other data is available regarding the role of IL-8 as prognostic/predictive biomarkers of relapse in patients with resected solid cancers.

In our meta-analysis, we considered a range of studies that provided data on the baseline values of IL-8 in different populations of NSCLC patients. However, other studies focused on the dynamic changes in IL-8 levels during treatment to elucidate its potential prognostic or predictive significance. In this light, in the prospective phase of this thesis, we observed a significant decrease in IL-8 levels among patients with advanced NSCLC responders to ICIs. Furthermore, Sanmamed et al. demonstrated that early changes in serum IL-8 levels, measured before radiologic evaluation, can predict treatment response and survival outcomes in patients receiving anti-PD-1 therapy for metastatic melanoma and NSCLC [200]. In particular, in the NSCLC cohort, responders exhibited a median decrease of 45.6% (Q1/Q3: -59.1 to -15.1), while non-responders showed a median increase of 27.0% (Q1-Q3: 8.3-52.1) (P < 0.0001). In addition, variations in IL-8 levels were observed to reflect tumor burden and could be used to identify pseudo-progression during ICI therapy [200]. Similar results were obtained by Zhao et al. [201]. The authors showed that lower levels of IL-6 (<5.4 pg/ml) and IL-8 (<20.6 pg/ml) after the third cycle of therapy were identified as independent risk factors for clinical benefit. Patients who experienced clinical benefit had significantly lower levels of IL-6 and IL-8 after the third treatment cycle. The odds ratio for clinical benefit was 0.402 (95% CI 0.191-0.848, P=0.016) for IL-6 and 0.776 (95% CI 0.633-0.951, P=0.015) for IL-8 [201]. These results suggest

that lower levels of IL-6 and IL-8 after the third cycle of therapy are associated with a higher likelihood of clinical benefit.

The prognostic role of IL-8 has also been evaluated in different tumor histologies treated with other therapeutic approaches. A retrospective study focusing on metastatic urothelial cancer and metastatic renal cell carcinomas demonstrated that higher baseline serum levels of IL-8 were linked to poorer OS in patients who received atezolizumab monotherapy or a combination of chemotherapy and atezolizumab but not in those treated with atezolizumab/bevacizumab and TKIs [164]. The study of Schalper et al., included in the meta-analysis, also involving patients with advanced renal cell carcinoma and melanoma who received immunotherapy, chemotherapy, or mTOR inhibitors, demonstrated a negative correlation between elevated serum levels of IL-8 and OS [163].

The evolving landscape of therapeutic approaches for NSCLC, particularly in the early stages, is witnessing a significant shift. Immunotherapies such as nivolumab [202], durvalumab [203] (in combination with chemotherapy), and atezolizumab [204], along with EGFR-TKIs [205,206], emerged as promising treatment options in (neo)adjuvant setting. In this light, identifying the role of IL-8 and other cytokines can provide valuable insights into disease relapse, treatment response, and potential therapeutic targets. By studying IL-8 levels and their correlation with treatment outcomes, further studies could determine if IL-8 may serve as a predictive marker for identifying patients who are more likely to benefit from these therapies or potential biomarkers for early detection of recurrence.

Targeting pathways involving immunosuppressive factors within the tumor microenvironment (TME) [207] may present an opportunity to augment the efficacy of immunotherapy. By disrupting the signaling pathways involved in the recruitment of immunosuppressive myeloid cells, such as MDSC and immature granulocytes, including IL-8, it is possible to enhance the overall efficacy of ICI. In this context, a novel study [NCT04123379] is currently recruiting NSCLC patients to evaluate if nivolumab with CCR2/5-inhibitor or anti-IL-8 before and after surgery may increase the immune response against the tumor and improve long-term survival rates.

5. CONCLUSION

In conclusion, this thesis not only indicates that the clinical impact of ICI promotes modulation of the immune landscape by limiting systemic inflammation and controlling MDSC-dependent immunosuppression but also demonstrates, through a metanalysis, the negative prognostic impact of the high levels of IL-8 in lung cancer, in particular in those patients treated with immunotherapy.

6. REFERENCES

1. AIOM (Associazione Italiana di Oncologia Medica), Linee guida AIOM "NEOPLASIE DEL POLMONE", ott. 2021. 2021.
2. Crispo A, Brennan P, Jöckel KH, et al. The cumulative risk of lung cancer among current, ex- and never-smokers in European men. Br J Cancer. 2004 Oct 4;91(7):1280-6.
3. Siegel RL, Miller KD, Wagle NS, et al. Cancer statistics, 2023. CA: A Cancer Journal for Clinicians. 2023;73(1):17-48.
4. Alberg AJ, Brock MV, Samet JM. Epidemiology of lung cancer: looking to the future. J Clin Oncol. 2005 May 10;23(14):3175-85.
5. Jha P, Peto R. Global Effects of Smoking, of Quitting, and of Taxing Tobacco. New England Journal of Medicine. 2014;370(1):60-68.
6. Zhong L, Goldberg MS, Parent ME, et al. Exposure to environmental tobacco smoke and the risk of lung cancer: a meta-analysis. Lung Cancer. 2000 Jan;27(1):3-18.
7. Taylor R, Najafi F, Dobson A. Meta-analysis of studies of passive smoking and lung cancer: effects of study type and continent. Int J Epidemiol. 2007 Oct;36(5):1048-59.
8. Gharibvand L, Shavlik D, Ghamsary M, et al. The Association between Ambient Fine Particulate Air Pollution and Lung Cancer Incidence: Results from the AHSMOG-2 Study. Environ Health Perspect. 2017 Mar;125(3):378-384.
9. Raaschou-Nielsen O, Andersen ZJ, Beelen R, et al. Air pollution and lung cancer incidence in 17 European cohorts: prospective analyses from the European Study of Cohorts for Air Pollution Effects (ESCAPE). Lancet Oncol. 2013 Aug;14(9):813-22.
10. Yokota J, Shiraishi K, Kohno T. Genetic basis for susceptibility to lung cancer: Recent progress and future directions. Adv Cancer Res. 2010;109:51-72.
11. WHO, WHO Classification of Tumours: Thoracic Tumours, 5°. Lyon: IARC, 2022. Consultato: 01 dicembre 2023. [Online]. 2022.
12. Postmus PE, Kerr KM, Oudkerk M, et al. Early and locally advanced non-small-cell lung cancer (NSCLC): ESMO Clinical Practice Guidelines for diagnosis, treatment and follow-up. Ann Oncol. 2017 Jul 1;28(suppl_4):iv1-iv21.
13. Ruilong Z, Daohai X, Li G, et al. Diagnostic value of 18F-FDG-PET/CT for the evaluation of solitary pulmonary nodules: a systematic review and meta-analysis. Nucl Med Commun. 2017 Jan;38(1):67-75.
14. Madsen PH, Holdgaard PC, Christensen JB, et al. Clinical utility of F-18 FDG PET-CT in the initial evaluation of lung cancer. Eur J Nucl Med Mol Imaging. 2016 Oct;43(11):2084-97.
15. Mena E, Yanamadala A, Cheng G, et al. The Current and Evolving Role of PET in Personalized Management of Lung Cancer. PET Clin. 2016 Jul;11(3):243-59.
16. Kao CH, Hsieh JF, Tsai SC, et al. Comparison and discrepancy of 18F-2-deoxyglucose positron emission tomography and Tc-99m MDP bone scan to detect bone metastases. Anticancer Res. 2000 May-Jun;20(3b):2189-92.
17. Kumar R, Xiu Y, Yu JQ, et al. 18F-FDG PET in evaluation of adrenal lesions in patients with lung cancer. J Nucl Med. 2004 Dec;45(12):2058-62.
18. Wu Y, Li P, Zhang H, et al. Diagnostic value of fluorine 18 fluorodeoxyglucose positron emission tomography/computed tomography for the detection of metastases in non-small-cell lung cancer patients. Int J Cancer. 2013 Jan 15;132(2):E37-47.

19. Chang MC, Chen JH, Liang JA, et al. Meta-analysis: comparison of F-18 fluorodeoxyglucose-positron emission tomography and bone scintigraphy in the detection of bone metastasis in patients with lung cancer. Acad Radiol. 2012 Mar;19(3):349-57.
20. Silvestri GA, Gonzalez AV, Jantz MA, et al. Methods for staging non-small cell lung cancer: Diagnosis and management of lung cancer, 3rd ed: American College of Chest Physicians evidence-based clinical practice guidelines. Chest. 2013 May;143(5 Suppl):e211S-e250S.
21. Vilmann P, Clementsen PF, Colella S, et al. Combined endobronchial and esophageal endosonography for the diagnosis and staging of lung cancer: European Society of Gastrointestinal Endoscopy (ESGE) Guideline, in cooperation with the European Respiratory Society (ERS) and the European Society of Thoracic Surgeons (ESTS). Endoscopy. 2015 Jun;47(6):545-59.
22. Trisolini R, Natali F, Fois A. Up-to date role of interventional pulmonology in the diagnosis and staging of non-small-cell lung cancer. Shanghai Chest. 2017;1:50-50.
23. Rivera MP, Mehta AC, Wahidi MM. Establishing the diagnosis of lung cancer: Diagnosis and management of lung cancer, 3rd ed: American College of Chest Physicians evidence-based clinical practice guidelines. Chest. 2013 May;143(5 Suppl):e142S-e165S.
24. Almeida FA, Salam S, Mehta AC, et al. Sampling Utility of the Convex Probe Endobronchial Ultrasound Visible Intrapulmonary Lesion. J Bronchology Interv Pulmonol. 2018 Oct;25(4):290-299.
25. Kuijvenhoven JC, Livi V, Morandi L, et al. The expanding role of endobronchial ultrasound in patients with centrally located intrapulmonary tumors. Lung Cancer. 2019 Aug;134:194-201.
26. Korevaar DA, Colella S, Spijker R, et al. Esophageal Endosonography for the Diagnosis of Intrapulmonary Tumors: A Systematic Review and Meta-Analysis. Respiration. 2017;93(2):126-137.
27. Wang Memoli JS, Nietert PJ, Silvestri GA. Meta-analysis of guided bronchoscopy for the evaluation of the pulmonary nodule. Chest. 2012 Aug;142(2):385-393.
28. Choi SH, Chae EJ, Kim JE, et al. Percutaneous CT-guided aspiration and core biopsy of pulmonary nodules smaller than 1 cm: analysis of outcomes of 305 procedures from a tertiary referral center. AJR Am J Roentgenol. 2013 Nov;201(5):964-70.
29. Takeshita J, Masago K, Kato R, et al. CT-guided fine-needle aspiration and core needle biopsies of pulmonary lesions: a single-center experience with 750 biopsies in Japan. AJR Am J Roentgenol. 2015 Jan;204(1):29-34.
30. Dhooria S, Aggarwal AN, Gupta D, et al. Utility and Safety of Endoscopic Ultrasound With Bronchoscope-Guided Fine-Needle Aspiration in Mediastinal Lymph Node Sampling: Systematic Review and Meta-Analysis. Respir Care. 2015 Jul;60(7):1040-50.
31. Livi V, Paioli D, Cancellieri A, et al. Diagnosis and Molecular Profiling of Lung Cancer by Percutaneous Ultrasound-Guided Biopsy of Superficial Metastatic Sites Is Safe and Highly Effective. Respiration. 2021;100(6):515-522.
32. Rami-Porta R, Bolejack V, Crowley J, et al. The IASLC Lung Cancer Staging Project: Proposals for the Revisions of the T Descriptors in the Forthcoming Eighth Edition of the TNM Classification for Lung Cancer. J Thorac Oncol. 2015 Jul;10(7):990-1003.
33. Asamura H, Chansky K, Crowley J, et al. The International Association for the Study of Lung Cancer Lung Cancer Staging Project: Proposals for the Revision

of the N Descriptors in the Forthcoming 8th Edition of the TNM Classification for Lung Cancer. J Thorac Oncol. 2015 Dec;10(12):1675-84.
34. Eberhardt WE, Mitchell A, Crowley J, et al. The IASLC Lung Cancer Staging Project: Proposals for the Revision of the M Descriptors in the Forthcoming Eighth Edition of the TNM Classification of Lung Cancer. J Thorac Oncol. 2015 Nov;10(11):1515-22.
35. Goldstraw P, Chansky K, Crowley J, et al. The IASLC Lung Cancer Staging Project: Proposals for Revision of the TNM Stage Groupings in the Forthcoming (Eighth) Edition of the TNM Classification for Lung Cancer. J Thorac Oncol. 2016 Jan;11(1):39-51.
36. Chansky K, Detterbeck FC, Nicholson AG, et al. The IASLC Lung Cancer Staging Project: External Validation of the Revision of the TNM Stage Groupings in the Eighth Edition of the TNM Classification of Lung Cancer. J Thorac Oncol. 2017 Jul;12(7):1109-1121.
37. Hendriks LE, Kerr KM, Menis J, et al. Oncogene-addicted metastatic non-small-cell lung cancer: ESMO Clinical Practice Guideline for diagnosis, treatment and follow-up. Ann Oncol. 2023 Apr;34(4):339-357.
38. Hendriks LE, Kerr KM, Menis J, et al. Non-oncogene-addicted metastatic non-small-cell lung cancer: ESMO Clinical Practice Guideline for diagnosis, treatment and follow-up. Ann Oncol. 2023 Apr;34(4):358-376.
39. Planchard D, Smit EF, Groen HJM, et al. Dabrafenib plus trametinib in patients with previously untreated BRAF(V600E)-mutant metastatic non-small-cell lung cancer: an open-label, phase 2 trial. Lancet Oncol. 2017 Oct;18(10):1307-1316.
40. Malapelle U, Sirera R, Jantus-Lewintre E, et al. Profile of the Roche cobas® EGFR mutation test v2 for non-small cell lung cancer. Expert Rev Mol Diagn. 2017 Mar;17(3):209-215.
41. Lynch TJ, Bell DW, Sordella R, et al. Activating Mutations in the Epidermal Growth Factor Receptor Underlying Responsiveness of Non–Small-Cell Lung Cancer to Gefitinib. New England Journal of Medicine. 2004;350(21):2129-2139.
42. Mok TS, Wu Y-L, Thongprasert S, et al. Gefitinib or Carboplatin–Paclitaxel in Pulmonary Adenocarcinoma. New England Journal of Medicine. 2009;361(10):947-957.
43. Rosell R, Carcereny E, Gervais R, et al. Erlotinib versus standard chemotherapy as first-line treatment for European patients with advanced EGFR mutation-positive non-small-cell lung cancer (EURTAC): a multicentre, open-label, randomised phase 3 trial. Lancet Oncol. 2012 Mar;13(3):239-46.
44. Soria J-C, Ohe Y, Vansteenkiste J, et al. Osimertinib in UntreatedEGFR-Mutated Advanced Non–Small-Cell Lung Cancer. New England Journal of Medicine. 2018;378(2):113-125.
45. Mok TS, Cheng Y, Zhou X, et al. Improvement in Overall Survival in a Randomized Study That Compared Dacomitinib With Gefitinib in Patients With Advanced Non-Small-Cell Lung Cancer and EGFR-Activating Mutations. J Clin Oncol. 2018 Aug 1;36(22):2244-2250.
46. Soda M, Choi YL, Enomoto M, et al. Identification of the transforming EML4-ALK fusion gene in non-small-cell lung cancer. Nature. 2007 Aug 2;448(7153):561-6.
47. Solomon BJ, Mok T, Kim DW, et al. First-line crizotinib versus chemotherapy in ALK-positive lung cancer. N Engl J Med. 2014 Dec 4;371(23):2167-77.
48. Peters S, Camidge DR, Shaw AT, et al. Alectinib versus Crizotinib in Untreated ALK-Positive Non-Small-Cell Lung Cancer. N Engl J Med. 2017 Aug 31;377(9):829-838.

49. Solomon BJ, Besse B, Bauer TM, et al. Lorlatinib in patients with ALK-positive non-small-cell lung cancer: results from a global phase 2 study. Lancet Oncol. 2018 Dec;19(12):1654-1667.
50. Camidge DR, Kim HR, Ahn MJ, et al. Brigatinib versus Crizotinib in ALK-Positive Non-Small-Cell Lung Cancer. N Engl J Med. 2018 Nov 22;379(21):2027-2039.
51. Shaw AT, Ou S-HI, Bang Y-J, et al. Crizotinib in ROS1-Rearranged Non–Small-Cell Lung Cancer. New England Journal of Medicine. 2014;371(21):1963-1971.
52. Dziadziuszko R, Krebs MG, De Braud F, et al. Updated Integrated Analysis of the Efficacy and Safety of Entrectinib in Locally Advanced or Metastatic ROS1 Fusion-Positive Non-Small-Cell Lung Cancer. J Clin Oncol. 2021 Apr 10;39(11):1253-1263.
53. Doebele RC, Drilon A, Paz-Ares L, et al. Entrectinib in patients with advanced or metastatic NTRK fusion-positive solid tumours: integrated analysis of three phase 1-2 trials. Lancet Oncol. 2020 Feb;21(2):271-282.
54. Reck M, Rodríguez-Abreu D, Robinson AG, et al. Pembrolizumab versus Chemotherapy for PD-L1–Positive Non–Small-Cell Lung Cancer. New England Journal of Medicine. 2016;375(19):1823-1833.
55. Yan TD, Black D, Bannon PG, et al. Systematic review and meta-analysis of randomized and nonrandomized trials on safety and efficacy of video-assisted thoracic surgery lobectomy for early-stage non-small-cell lung cancer. J Clin Oncol. 2009 May 20;27(15):2553-62.
56. Villamizar NR, Darrabie MD, Burfeind WR, et al. Thoracoscopic lobectomy is associated with lower morbidity compared with thoracotomy. J Thorac Cardiovasc Surg. 2009 Aug;138(2):419-25.
57. Howington JA, Blum MG, Chang AC, et al. Treatment of stage I and II non-small cell lung cancer: Diagnosis and management of lung cancer, 3rd ed: American College of Chest Physicians evidence-based clinical practice guidelines. Chest. 2013 May;143(5 Suppl):e278S-e313S.
58. Ball D, Mai GT, Vinod S, et al. Stereotactic ablative radiotherapy versus standard radiotherapy in stage 1 non-small-cell lung cancer (TROG 09.02 CHISEL): a phase 3, open-label, randomised controlled trial. Lancet Oncol. 2019 Apr;20(4):494-503.
59. Li C, Wang L, Wu Q, et al. A meta-analysis comparing stereotactic body radiotherapy vs conventional radiotherapy in inoperable stage I non-small cell lung cancer. Medicine (Baltimore). 2020 Aug 21;99(34):e21715.
60. Pignon J-P, Tribodet H, Scagliotti GV, et al. Lung Adjuvant Cisplatin Evaluation: A Pooled Analysis by the LACE Collaborative Group. Journal of Clinical Oncology. 2008;26(21):3552-3559.
61. Burdett S, Pignon JP, Tierney J, et al. Adjuvant chemotherapy for resected early-stage non-small cell lung cancer. Cochrane Database Syst Rev. 2015 Mar 2;2015(3):Cd011430.
62. Preoperative chemotherapy for non-small-cell lung cancer: a systematic review and meta-analysis of individual participant data. The Lancet. 2014;383(9928):1561-1571.
63. Zhang Y, Hu X, Liu D, et al. Effectiveness of neoadjuvant chemotherapy on the survival outcomes of patients with resectable non-small-cell lung cancer: A meta-analysis of randomized controlled trials. Surg Oncol. 2021 Sep;38:101590.
64. Sakib N, Li N, Zhu X, et al. Effect of postoperative radiotherapy on outcome in resectable stage IIIA-N2 non-small-cell lung cancer: an updated meta-analysis. Nucl Med Commun. 2018 Jan;39(1):51-59.

65. Juan O, Popat S. Ablative Therapy for Oligometastatic Non-Small Cell Lung Cancer. Clin Lung Cancer. 2017 Nov;18(6):595-606.
66. Spigel DR, Faivre-Finn C, Gray JE, et al. Five-Year Survival Outcomes From the PACIFIC Trial: Durvalumab After Chemoradiotherapy in Stage III Non-Small-Cell Lung Cancer. J Clin Oncol. 2022 Apr 20;40(12):1301-1311.
67. Reck M, Rodríguez-Abreu D, Robinson AG, et al. Five-Year Outcomes With Pembrolizumab Versus Chemotherapy for Metastatic Non-Small-Cell Lung Cancer With PD-L1 Tumor Proportion Score ≥ 50. J Clin Oncol. 2021 Jul 20;39(21):2339-2349.
68. Sezer A, Kilickap S, Gümüş M, et al. Cemiplimab monotherapy for first-line treatment of advanced non-small-cell lung cancer with PD-L1 of at least 50%: a multicentre, open-label, global, phase 3, randomised, controlled trial. The Lancet. 2021;397(10274):592-604.
69. Herbst RS, Giaccone G, De Marinis F, et al. Atezolizumab for First-Line Treatment of PD-L1–Selected Patients with NSCLC. New England Journal of Medicine. 2020;383(14):1328-1339.
70. Gadgeel S, Rodríguez-Abreu D, Speranza G, et al. Updated Analysis From KEYNOTE-189: Pembrolizumab or Placebo Plus Pemetrexed and Platinum for Previously Untreated Metastatic Nonsquamous Non-Small-Cell Lung Cancer. J Clin Oncol. 2020 May 10;38(14):1505-1517.
71. Novello S, Kowalski DM, Luft A, et al. Pembrolizumab Plus Chemotherapy in Squamous Non-Small-Cell Lung Cancer: 5-Year Update of the Phase III KEYNOTE-407 Study. J Clin Oncol. 2023 Apr 10;41(11):1999-2006.
72. Reck M, Ciuleanu TE, Cobo M, et al. First-line nivolumab plus ipilimumab with two cycles of chemotherapy versus chemotherapy alone (four cycles) in advanced non-small-cell lung cancer: CheckMate 9LA 2-year update. ESMO Open. 2021 Oct;6(5):100273.
73. Scagliotti GV, Parikh P, von Pawel J, et al. Phase III study comparing cisplatin plus gemcitabine with cisplatin plus pemetrexed in chemotherapy-naive patients with advanced-stage non-small-cell lung cancer. J Clin Oncol. 2008 Jul 20;26(21):3543-51.
74. Paz-Ares L, de Marinis F, Dediu M, et al. Maintenance therapy with pemetrexed plus best supportive care versus placebo plus best supportive care after induction therapy with pemetrexed plus cisplatin for advanced non-squamous non-small-cell lung cancer (PARAMOUNT): a double-blind, phase 3, randomised controlled trial. Lancet Oncol. 2012 Mar;13(3):247-55.
75. Paz-Ares LG, de Marinis F, Dediu M, et al. PARAMOUNT: Final overall survival results of the phase III study of maintenance pemetrexed versus placebo immediately after induction treatment with pemetrexed plus cisplatin for advanced nonsquamous non-small-cell lung cancer. J Clin Oncol. 2013 Aug 10;31(23):2895-902.
76. Shepherd FA, Dancey J, Ramlau R, et al. Prospective randomized trial of docetaxel versus best supportive care in patients with non-small-cell lung cancer previously treated with platinum-based chemotherapy. J Clin Oncol. 2000 May;18(10):2095-103.
77. Fossella FV, DeVore R, Kerr RN, et al. Randomized phase III trial of docetaxel versus vinorelbine or ifosfamide in patients with advanced non-small-cell lung cancer previously treated with platinum-containing chemotherapy regimens. The TAX 320 Non-Small Cell Lung Cancer Study Group. J Clin Oncol. 2000 Jun;18(12):2354-62.
78. Brahmer J, Reckamp KL, Baas P, et al. Nivolumab versus Docetaxel in Advanced Squamous-Cell Non–Small-Cell Lung Cancer. New England Journal of Medicine. 2015;373(2):123-135.

79. Borghaei H, Gettinger S, Vokes EE, et al. Five-Year Outcomes From the Randomized, Phase III Trials CheckMate 017 and 057: Nivolumab Versus Docetaxel in Previously Treated Non-Small-Cell Lung Cancer. J Clin Oncol. 2021 Mar 1;39(7):723-733.
80. Herbst RS, Baas P, Kim DW, et al. Pembrolizumab versus docetaxel for previously treated, PD-L1-positive, advanced non-small-cell lung cancer (KEYNOTE-010): a randomised controlled trial. Lancet. 2016 Apr 9;387(10027):1540-1550.
81. Rittmeyer A, Barlesi F, Waterkamp D, et al. Atezolizumab versus docetaxel in patients with previously treated non-small-cell lung cancer (OAK): a phase 3, open-label, multicentre randomised controlled trial. Lancet. 2017 Jan 21;389(10066):255-265.
82. Reck M, Kaiser R, Mellemgaard A, et al. Docetaxel plus nintedanib versus docetaxel plus placebo in patients with previously treated non-small-cell lung cancer (LUME-Lung 1): a phase 3, double-blind, randomised controlled trial. Lancet Oncol. 2014 Feb;15(2):143-55.
83. Novello S, Kaiser R, Mellemgaard A, et al. Analysis of patient-reported outcomes from the LUME-Lung 1 trial: a randomised, double-blind, placebo-controlled, Phase III study of second-line nintedanib in patients with advanced non-small cell lung cancer. Eur J Cancer. 2015 Feb;51(3):317-26.
84. Effects of vinorelbine on quality of life and survival of elderly patients with advanced non-small-cell lung cancer. The Elderly Lung Cancer Vinorelbine Italian Study Group. J Natl Cancer Inst. 1999 Jan 6;91(1):66-72.
85. Chen DS, Mellman I. Oncology meets immunology: the cancer-immunity cycle. Immunity. 2013 Jul 25;39(1):1-10.
86. Sharma P, Hu-Lieskovan S, Wargo JA, et al. Primary, Adaptive, and Acquired Resistance to Cancer Immunotherapy. Cell. 2017 Feb 9;168(4):707-723.
87. Maalej KM, Merhi M, Inchakalody VP, et al. CAR-cell therapy in the era of solid tumor treatment: current challenges and emerging therapeutic advances. Mol Cancer. 2023 Jan 30;22(1):20.
88. Krummel MF, Allison JP. CD28 and CTLA-4 have opposing effects on the response of T cells to stimulation. J Exp Med. 1995 Aug 1;182(2):459-65.
89. Malas S, Harrasser M, Lacy KE, et al. Antibody therapies for melanoma: new and emerging opportunities to activate immunity (Review). Oncol Rep. 2014 Sep;32(3):875-86.
90. Walunas TL, Lenschow DJ, Bakker CY, et al. CTLA-4 can function as a negative regulator of T cell activation. Immunity. 1994 Aug;1(5):405-13.
91. Hui E, Cheung J, Zhu J, et al. T cell costimulatory receptor CD28 is a primary target for PD-1-mediated inhibition. Science. 2017 Mar 31;355(6332):1428-1433.
92. Onoi K, Chihara Y, Uchino J, et al. Immune Checkpoint Inhibitors for Lung Cancer Treatment: A Review. J Clin Med. 2020 May 6;9(5).
93. Aguilar EJ, Ricciuti B, Gainor JF, et al. Outcomes to first-line pembrolizumab in patients with non-small-cell lung cancer and very high PD-L1 expression. Ann Oncol. 2019 Oct 1;30(10):1653-1659.
94. Socinski MA, Jotte RM, Cappuzzo F, et al. Atezolizumab for First-Line Treatment of Metastatic Nonsquamous NSCLC. N Engl J Med. 2018 Jun 14;378(24):2288-2301.
95. Mok TSK, Wu YL, Kudaba I, et al. Pembrolizumab versus chemotherapy for previously untreated, PD-L1-expressing, locally advanced or metastatic non-small-cell lung cancer (KEYNOTE-042): a randomised, open-label, controlled, phase 3 trial. Lancet. 2019 May 4;393(10183):1819-1830.

96. Park S, Choi YD, Kim J, et al. Efficacy of immune checkpoint inhibitors according to PD-L1 tumor proportion scores in non-small cell lung cancer. Thorac Cancer. 2020 Feb;11(2):408-414.
97. Gibbons DL, Byers LA, Kurie JM. Smoking, p53 mutation, and lung cancer. Mol Cancer Res. 2014 Jan;12(1):3-13.
98. Shitara K, Özgüroğlu M, Bang YJ, et al. Pembrolizumab versus paclitaxel for previously treated, advanced gastric or gastro-oesophageal junction cancer (KEYNOTE-061): a randomised, open-label, controlled, phase 3 trial. Lancet. 2018 Jul 14;392(10142):123-133.
99. Mezquita L, Auclin E, Ferrara R, et al. Association of the Lung Immune Prognostic Index With Immune Checkpoint Inhibitor Outcomes in Patients With Advanced Non-Small Cell Lung Cancer. JAMA Oncol. 2018 Mar 1;4(3):351-357.
100. Veglia F, Perego M, Gabrilovich D. Myeloid-derived suppressor cells coming of age. Nat Immunol. 2018 Feb;19(2):108-119.
101. Gabrilovich DI, Ostrand-Rosenberg S, Bronte V. Coordinated regulation of myeloid cells by tumours. Nat Rev Immunol. 2012 Mar 22;12(4):253-68.
102. Marvel D, Gabrilovich DI. Myeloid-derived suppressor cells in the tumor microenvironment: expect the unexpected. J Clin Invest. 2015 Sep;125(9):3356-64.
103. Kruger P, Saffarzadeh M, Weber AN, et al. Neutrophils: Between host defence, immune modulation, and tissue injury. PLoS Pathog. 2015 Mar;11(3):e1004651.
104. Shi C, Pamer EG. Monocyte recruitment during infection and inflammation. Nat Rev Immunol. 2011 Oct 10;11(11):762-74.
105. Landskron G, De la Fuente M, Thuwajit P, et al. Chronic inflammation and cytokines in the tumor microenvironment. J Immunol Res. 2014;2014:149185.
106. Umansky V, Blattner C, Gebhardt C, et al. The Role of Myeloid-Derived Suppressor Cells (MDSC) in Cancer Progression. Vaccines (Basel). 2016 Nov 3;4(4).
107. Youn JI, Collazo M, Shalova IN, et al. Characterization of the nature of granulocytic myeloid-derived suppressor cells in tumor-bearing mice. J Leukoc Biol. 2012 Jan;91(1):167-81.
108. Bronte V, Brandau S, Chen S-H, et al. Recommendations for myeloid-derived suppressor cell nomenclature and characterization standards. Nature Communications. 2016;7(1):12150.
109. Netea MG, Joosten LA, Latz E, et al. Trained immunity: A program of innate immune memory in health and disease. Science. 2016 Apr 22;352(6284):aaf1098.
110. Condamine T, Gabrilovich DI. Molecular mechanisms regulating myeloid-derived suppressor cell differentiation and function. Trends Immunol. 2011 Jan;32(1):19-25.
111. Bronte V, Chappell DB, Apolloni E, et al. Unopposed production of granulocyte-macrophage colony-stimulating factor by tumors inhibits CD8+ T cell responses by dysregulating antigen-presenting cell maturation. J Immunol. 1999 May 15;162(10):5728-37.
112. Dolcetti L, Peranzoni E, Ugel S, et al. Hierarchy of immunosuppressive strength among myeloid-derived suppressor cell subsets is determined by GM-CSF. Eur J Immunol. 2010 Jan;40(1):22-35.
113. Umansky V, Sevko A. Tumor microenvironment and myeloid-derived suppressor cells. Cancer Microenviron. 2013 Aug;6(2):169-77.
114. Yan D, Yang Q, Shi M, et al. Polyunsaturated fatty acids promote the expansion of myeloid-derived suppressor cells by activating the JAK/STAT3 pathway. Eur J Immunol. 2013 Nov;43(11):2943-55.

115. Haverkamp JM, Smith AM, Weinlich R, et al. Myeloid-derived suppressor activity is mediated by monocytic lineages maintained by continuous inhibition of extrinsic and intrinsic death pathways. Immunity. 2014 Dec 18;41(6):947-59.
116. Condamine T, Mastio J, Gabrilovich DI. Transcriptional regulation of myeloid-derived suppressor cells. J Leukoc Biol. 2015 Dec;98(6):913-22.
117. Mandruzzato S, Brandau S, Britten CM, et al. Toward harmonized phenotyping of human myeloid-derived suppressor cells by flow cytometry: results from an interim study. Cancer Immunol Immunother. 2016 Feb;65(2):161-9.
118. Krishnamoorthy M, Gerhardt L, Maleki Vareki S. Immunosuppressive Effects of Myeloid-Derived Suppressor Cells in Cancer and Immunotherapy. Cells. 2021 May 11;10(5).
119. Gabrilovich DI. Myeloid-Derived Suppressor Cells. Cancer Immunol Res. 2017 Jan;5(1):3-8.
120. Kwak T, Wang F, Deng H, et al. Distinct Populations of Immune-Suppressive Macrophages Differentiate from Monocytic Myeloid-Derived Suppressor Cells in Cancer. Cell Rep. 2020 Dec 29;33(13):108571.
121. Hart KM, Byrne KT, Molloy MJ, et al. IL-10 immunomodulation of myeloid cells regulates a murine model of ovarian cancer. Front Immunol. 2011;2:29.
122. Sinha P, Okoro C, Foell D, et al. Proinflammatory S100 proteins regulate the accumulation of myeloid-derived suppressor cells. J Immunol. 2008 Oct 1;181(7):4666-75.
123. Hoechst B, Ormandy LA, Ballmaier M, et al. A new population of myeloid-derived suppressor cells in hepatocellular carcinoma patients induces CD4(+)CD25(+)Foxp3(+) T cells. Gastroenterology. 2008 Jul;135(1):234-43.
124. Kehrl JH, Roberts AB, Wakefield LM, et al. Transforming growth factor beta is an important immunomodulatory protein for human B lymphocytes. J Immunol. 1986 Dec 15;137(12):3855-60.
125. Brabletz T, Pfeuffer I, Schorr E, et al. Transforming growth factor beta and cyclosporin A inhibit the inducible activity of the interleukin-2 gene in T cells through a noncanonical octamer-binding site. Mol Cell Biol. 1993 Feb;13(2):1155-62.
126. Thomas DA, Massagué J. TGF-beta directly targets cytotoxic T cell functions during tumor evasion of immune surveillance. Cancer Cell. 2005 Nov;8(5):369-80.
127. Synnestvedt K, Furuta GT, Comerford KM, et al. Ecto-5'-nucleotidase (CD73) regulation by hypoxia-inducible factor-1 mediates permeability changes in intestinal epithelia. J Clin Invest. 2002 Oct;110(7):993-1002.
128. Morello S, Pinto A, Blandizzi C, et al. Myeloid cells in the tumor microenvironment: Role of adenosine. Oncoimmunology. 2016 Mar;5(3):e1108515.
129. Corzo CA, Condamine T, Lu L, et al. HIF-1α regulates function and differentiation of myeloid-derived suppressor cells in the tumor microenvironment. J Exp Med. 2010 Oct 25;207(11):2439-53.
130. Rodriguez PC, Quiceno DG, Ochoa AC. L-arginine availability regulates T-lymphocyte cell-cycle progression. Blood. 2007 Feb 15;109(4):1568-73.
131. Bronte V, Zanovello P. Regulation of immune responses by L-arginine metabolism. Nat Rev Immunol. 2005 Aug;5(8):641-54.
132. Rodriguez PC, Quiceno DG, Zabaleta J, et al. Arginase I production in the tumor microenvironment by mature myeloid cells inhibits T-cell receptor expression and antigen-specific T-cell responses. Cancer Res. 2004 Aug 15;64(16):5839-49.
133. Grohmann U, Fallarino F, Bianchi R, et al. A defect in tryptophan catabolism impairs tolerance in nonobese diabetic mice. J Exp Med. 2003 Jul 7;198(1):153-60.

134. Yu J, Du W, Yan F, et al. Myeloid-derived suppressor cells suppress antitumor immune responses through IDO expression and correlate with lymph node metastasis in patients with breast cancer. J Immunol. 2013 Apr 1;190(7):3783-97.
135. Munn DH, Sharma MD, Baban B, et al. GCN2 kinase in T cells mediates proliferative arrest and anergy induction in response to indoleamine 2,3-dioxygenase. Immunity. 2005 May;22(5):633-42.
136. Fallarino F, Grohmann U, You S, et al. The combined effects of tryptophan starvation and tryptophan catabolites down-regulate T cell receptor zeta-chain and induce a regulatory phenotype in naive T cells. J Immunol. 2006 Jun 1;176(11):6752-61.
137. Metz R, Rust S, Duhadaway JB, et al. IDO inhibits a tryptophan sufficiency signal that stimulates mTOR: A novel IDO effector pathway targeted by D-1-methyl-tryptophan. Oncoimmunology. 2012 Dec 1;1(9):1460-1468.
138. Zanin-Zhorov A, Ding Y, Kumari S, et al. Protein kinase C-theta mediates negative feedback on regulatory T cell function. Science. 2010 Apr 16;328(5976):372-6.
139. Mezrich JD, Fechner JH, Zhang X, et al. An interaction between kynurenine and the aryl hydrocarbon receptor can generate regulatory T cells. J Immunol. 2010 Sep 15;185(6):3190-8.
140. Liu Y, Liang X, Dong W, et al. Tumor-Repopulating Cells Induce PD-1 Expression in CD8(+) T Cells by Transferring Kynurenine and AhR Activation. Cancer Cell. 2018 Mar 12;33(3):480-494.e7.
141. Yang J, Anholts J, Kolbe U, et al. Calcium-Binding Proteins S100A8 and S100A9: Investigation of Their Immune Regulatory Effect in Myeloid Cells. Int J Mol Sci. 2018 Jun 21;19(7).
142. Schmielau J, Finn OJ. Activated granulocytes and granulocyte-derived hydrogen peroxide are the underlying mechanism of suppression of t-cell function in advanced cancer patients. Cancer Res. 2001 Jun 15;61(12):4756-60.
143. Gehad AE, Lichtman MK, Schmults CD, et al. Nitric oxide-producing myeloid-derived suppressor cells inhibit vascular E-selectin expression in human squamous cell carcinomas. J Invest Dermatol. 2012 Nov;132(11):2642-51.
144. Molon B, Ugel S, Del Pozzo F, et al. Chemokine nitration prevents intratumoral infiltration of antigen-specific T cells. J Exp Med. 2011 Sep 26;208(10):1949-62.
145. Obermajer N, Muthuswamy R, Lesnock J, et al. Positive feedback between PGE2 and COX2 redirects the differentiation of human dendritic cells toward stable myeloid-derived suppressor cells. Blood. 2011 Nov 17;118(20):5498-505.
146. Sinha P, Clements VK, Fulton AM, et al. Prostaglandin E2 promotes tumor progression by inducing myeloid-derived suppressor cells. Cancer Res. 2007 May 1;67(9):4507-13.
147. Kalluri R, Weinberg RA. The basics of epithelial-mesenchymal transition. J Clin Invest. 2009 Jun;119(6):1420-8.
148. Toh B, Wang X, Keeble J, et al. Mesenchymal transition and dissemination of cancer cells is driven by myeloid-derived suppressor cells infiltrating the primary tumor. PLoS Biol. 2011 Sep;9(9):e1001162.
149. Cui TX, Kryczek I, Zhao L, et al. Myeloid-derived suppressor cells enhance stemness of cancer cells by inducing microRNA101 and suppressing the corepressor CtBP2. Immunity. 2013 Sep 19;39(3):611-21.
150. Zhu J, Powis De Tenbossche CG, Cané S, et al. Resistance to cancer immunotherapy mediated by apoptosis of tumor-infiltrating lymphocytes. Nature Communications. 2017;8(1).
151. Meyer C, Cagnon L, Costa-Nunes CM, et al. Frequencies of circulating MDSC correlate with clinical outcome of melanoma patients treated with ipilimumab. Cancer Immunol Immunother. 2014 Mar;63(3):247-57.

152. Passaro A, Mancuso P, Gandini S, et al. Gr-MDSC-linked asset as a potential immune biomarker in pretreated NSCLC receiving nivolumab as second-line therapy. Clin Transl Oncol. 2020 Apr;22(4):603-611.
153. Gebhardt C, Sevko A, Jiang H, et al. Myeloid Cells and Related Chronic Inflammatory Factors as Novel Predictive Markers in Melanoma Treatment with Ipilimumab. Clin Cancer Res. 2015 Dec 15;21(24):5453-9.
154. Mariathasan S, Turley SJ, Nickles D, et al. TGFβ attenuates tumour response to PD-L1 blockade by contributing to exclusion of T cells. Nature. 2018;554(7693):544-548.
155. Li Z, Pang Y, Gara SK, et al. Gr-1+CD11b+ cells are responsible for tumor promoting effect of TGF-β in breast cancer progression. Int J Cancer. 2012 Dec 1;131(11):2584-95.
156. Bagnoli M, Canevari S, Mezzanzanica D. Cellular FLICE-inhibitory protein (c-FLIP) signalling: a key regulator of receptor-mediated apoptosis in physiologic context and in cancer. Int J Biochem Cell Biol. 2010 Feb;42(2):210-3.
157. Fiore A, Ugel S, De Sanctis F, et al. Induction of immunosuppressive functions and NF-κB by FLIP in monocytes. Nature Communications. 2018;9(1).
158. Musiu C, Caligola S, Fiore A, et al. Fatal cytokine release syndrome by an aberrant FLIP/STAT3 axis. Cell Death & Differentiation. 2022;29(2):420-438.
159. Suwinski R, Giglok M, Galwas-Kliber K, et al. Blood serum proteins as biomarkers for prediction of survival, locoregional control and distant metastasis rate in radiotherapy and radio-chemotherapy for non-small cell lung cancer. BMC Cancer. 2019 May 8;19(1):427.
160. Wu T, Yang W, Sun A, et al. The Role of CXC Chemokines in Cancer Progression. Cancers (Basel). 2022 Dec 28;15(1).
161. Waugh DJ, Wilson C. The interleukin-8 pathway in cancer. Clin Cancer Res. 2008 Nov 1;14(21):6735-41.
162. Abraham RT. Chemokine to the rescue: interleukin-8 mediates resistance to PI3K-pathway-targeted therapy in breast cancer. Cancer Cell. 2012 Dec 11;22(6):703-5.
163. Schalper KA, Carleton M, Zhou M, et al. Elevated serum interleukin-8 is associated with enhanced intratumor neutrophils and reduced clinical benefit of immune-checkpoint inhibitors. Nat Med. 2020 May;26(5):688-692.
164. Yuen KC, Liu LF, Gupta V, et al. High systemic and tumor-associated IL-8 correlates with reduced clinical benefit of PD-L1 blockade. Nat Med. 2020 May;26(5):693-698.
165. Bazzichetto C, Milella M, Zampiva I, et al. Interleukin-8 in Colorectal Cancer: A Systematic Review and Meta-Analysis of Its Potential Role as a Prognostic Biomarker. Biomedicines. 2022 Oct 19;10(10).
166. Kluger HM, Tawbi HA, Ascierto ML, et al. Defining tumor resistance to PD-1 pathway blockade: recommendations from the first meeting of the SITC Immunotherapy Resistance Taskforce. J Immunother Cancer. 2020 Mar;8(1).
167. Schoenfeld AJ, Antonia SJ, Awad MM, et al. Clinical definition of acquired resistance to immunotherapy in patients with metastatic non-small-cell lung cancer. Ann Oncol. 2021 Dec;32(12):1597-1607.
168. Solito S, Pinton L, De Sanctis F, et al. Methods to Measure MDSC Immune Suppressive Activity In Vitro and In Vivo. Curr Protoc Immunol. 2019 Feb;124(1):e61.
169. Parks DR, Roederer M, Moore WA. A new “Logicle” display method avoids deceptive effects of logarithmic scaling for low signals and compensated data. Cytometry Part A. 2006;69A(6):541-551.

170. Page MJ, McKenzie JE, Bossuyt PM, et al. The PRISMA 2020 statement: an updated guideline for reporting systematic reviews. Bmj. 2021 Mar 29;372:n71.
171. DerSimonian R, Laird N. Meta-analysis in clinical trials revisited. Contemp Clin Trials. 2015 Nov;45(Pt A):139-45.
172. Ramos M, Geistlinger L, Oh S, et al. Multiomic Integration of Public Oncology Databases in Bioconductor. JCO Clin Cancer Inform. 2020 Oct;4:958-971.
173. Long H, Jia Q, Wang L, et al. Tumor-induced erythroid precursor-differentiated myeloid cells mediate immunosuppression and curtail anti-PD-1/PD-L1 treatment efficacy. Cancer Cell. 2022 Jun 13;40(6):674-693.e7.
174. Fidler MJ, Frankenberger C, Seto R, et al. Differential expression of circulating biomarkers of tumor phenotype and outcomes in previously treated non-small cell lung cancer patients receiving erlotinib vs. cytotoxic chemotherapy. Oncotarget. 2017 Aug 29;8(35):58108-58121.
175. Rice SJ, Belani CP. Diversity and heterogeneity of immune states in non-small cell lung cancer and small cell lung cancer. PLoS One. 2021;16(12):e0260988.
176. Cheng D, Kong H, Li Y. Prognostic values of VEGF and IL-8 in malignant pleural effusion in patients with lung cancer. Biomarkers. 2013 Aug;18(5):386-90.
177. Orditura M, De Vita F, Catalano G, et al. Elevated serum levels of interleukin-8 in advanced non-small cell lung cancer patients: relationship with prognosis. J Interferon Cytokine Res. 2002 Nov;22(11):1129-35.
178. Sui X, Jiang L, Teng H, et al. Prediction of Clinical Outcome in Locally Advanced Non-Small Cell Lung Cancer Patients Treated With Chemoradiotherapy by Plasma Markers. Front Oncol. 2020;10:625911.
179. Ryan BM, Pine SR, Chaturvedi AK, et al. A combined prognostic serum interleukin-8 and interleukin-6 classifier for stage 1 lung cancer in the prostate, lung, colorectal, and ovarian cancer screening trial. J Thorac Oncol. 2014 Oct;9(10):1494-503.
180. Zhou J, Chao Y, Yao D, et al. Impact of chronic obstructive pulmonary disease on immune checkpoint inhibitor efficacy in advanced lung cancer and the potential prognostic factors. Transl Lung Cancer Res. 2021 May;10(5):2148-2162.
181. Gu L, Yao Y, Chen Z. An inter-correlation among chemokine (C-X-C motif) ligand (CXCL) 1, CXCL2 and CXCL8, and their diversified potential as biomarkers for tumor features and survival profiles in non-small cell lung cancer patients. Transl Cancer Res. 2021 Feb;10(2):748-758.
182. Seike M, Yanaihara N, Bowman ED, et al. Use of a cytokine gene expression signature in lung adenocarcinoma and the surrounding tissue as a prognostic classifier. J Natl Cancer Inst. 2007 Aug 15;99(16):1257-69.
183. Viechtbauer W, Cheung MW. Outlier and influence diagnostics for meta-analysis. Res Synth Methods. 2010 Apr;1(2):112-25.
184. Siegel RL, Miller KD, Fuchs HE, et al. Cancer statistics, 2022. CA Cancer J Clin. 2022 Jan;72(1):7-33.
185. Marei HE, Hasan A, Pozzoli G, et al. Cancer immunotherapy with immune checkpoint inhibitors (ICIs): potential, mechanisms of resistance, and strategies for reinvigorating T cell responsiveness when resistance is acquired. Cancer Cell Int. 2023 Apr 10;23(1):64.
186. Zalaquett Z, Catherine Rita Hachem M, Kassis Y, et al. Acquired resistance mechanisms to osimertinib: The constant battle. Cancer Treat Rev. 2023 May;116:102557.
187. Liu H, Zhao Q, Tan L, et al. Neutralizing IL-8 potentiates immune checkpoint blockade efficacy for glioma. Cancer Cell. 2023 Apr 10;41(4):693-710.e8.

188. Hailemichael Y, Johnson DH, Abdel-Wahab N, et al. Interleukin-6 blockade abrogates immunotherapy toxicity and promotes tumor immunity. Cancer Cell. 2022 May 9;40(5):509-523.e6.
189. Li L, Liu YD, Zhan YT, et al. High levels of CCL2 or CCL4 in the tumor microenvironment predict unfavorable survival in lung adenocarcinoma. Thorac Cancer. 2018 Jul;9(7):775-784.
190. Kaplanov I, Carmi Y, Kornetsky R, et al. Blocking IL-1β reverses the immunosuppression in mouse breast cancer and synergizes with anti-PD-1 for tumor abrogation. Proc Natl Acad Sci U S A. 2019 Jan 22;116(4):1361-1369.
191. Musiu C, Caligola S, Fiore A, et al. Fatal cytokine release syndrome by an aberrant FLIP/STAT3 axis. Cell Death Differ. 2022 Feb;29(2):420-438.
192. Trovato R, Fiore A, Sartori S, et al. Immunosuppression by monocytic myeloid-derived suppressor cells in patients with pancreatic ductal carcinoma is orchestrated by STAT3. J Immunother Cancer. 2019 Sep 18;7(1):255.
193. Schad SE, Chow A, Mangarin L, et al. Tumor-induced double positive T cells display distinct lineage commitment mechanisms and functions. J Exp Med. 2022 Jun 6;219(6).
194. Harel M, Lahav C, Jacob E, et al. Longitudinal plasma proteomic profiling of patients with non-small cell lung cancer undergoing immune checkpoint blockade. J Immunother Cancer. 2022 Jun;10(6).
195. Mao XC, Yang CC, Yang YF, et al. Peripheral cytokine levels as novel predictors of survival in cancer patients treated with immune checkpoint inhibitors: A systematic review and meta-analysis. Front Immunol. 2022;13:884592.
196. McDermott DF, Huseni MA, Atkins MB, et al. Clinical activity and molecular correlates of response to atezolizumab alone or in combination with bevacizumab versus sunitinib in renal cell carcinoma. Nat Med. 2018 Jun;24(6):749-757.
197. Najjar YG, Rayman P, Jia X, et al. Myeloid-Derived Suppressor Cell Subset Accumulation in Renal Cell Carcinoma Parenchyma Is Associated with Intratumoral Expression of IL1β, IL8, CXCL5, and Mip-1α. Clin Cancer Res. 2017 May 1;23(9):2346-2355.
198. Alfaro C, Teijeira A, Oñate C, et al. Tumor-Produced Interleukin-8 Attracts Human Myeloid-Derived Suppressor Cells and Elicits Extrusion of Neutrophil Extracellular Traps (NETs). Clin Cancer Res. 2016 Aug 1;22(15):3924-36.
199. Mariathasan S, Turley SJ, Nickles D, et al. TGFβ attenuates tumour response to PD-L1 blockade by contributing to exclusion of T cells. Nature. 2018 Feb 22;554(7693):544-548.
200. Sanmamed MF, Perez-Gracia JL, Schalper KA, et al. Changes in serum interleukin-8 (IL-8) levels reflect and predict response to anti-PD-1 treatment in melanoma and non-small-cell lung cancer patients. Annals of Oncology. 2017;28(8):1988-1995.
201. Zhao N, Yi Y, Cao W, et al. Serum cytokine levels for predicting immune-related adverse events and the clinical response in lung cancer treated with immunotherapy. Front Oncol. 2022;12:923531.
202. Forde PM, Spicer J, Girard N, et al. 84O Neoadjuvant nivolumab (N) + platinum-doublet chemotherapy (C) for resectable NSCLC: 3-y update from CheckMate 816. Journal of Thoracic Oncology. 2023;18(4):S89-S90.
203. John V. Heymach DH, Tetsuya Mitsudomi, Janis M. Taube, Gabriella Galffy, Maximilian Hochmair, Thomas Winder, Ruslan Zukov, Gabriel Garbaos, Shugeng Gao, Hiroaki Kuroda, Jian You, Kang-Yun Lee, Lorenzo Antonuzzo, Mike Aperghis, Gary J. Doherty, Helen Mann, Tamer M. Fouad, Martin Reck. CT005 - AEGEAN: A phase 3 trial of neoadjuvant durvalumab + chemotherapy followed by adjuvant durvalumab in patients with resectable NSCLC

[Proceedings of the 114th Annual Meeting of the American Association for Cancer Research]. 2023 2023 April 14-19.
204. Wakelee H, Altorki N, Felip E, et al. PL03.09 IMpower010:Overall Survival Interim Analysis of a Phase III Study of Atezolizumab vs Best Supportive Care in Resected NSCLC. Journal of Thoracic Oncology. 2022 2022/09/01/;17(9, Supplement):S2.
205. Herbst RS, Wu Y-L, John T, et al. Adjuvant Osimertinib for Resected EGFR-Mutated Stage IB-IIIA Non–Small-Cell Lung Cancer: Updated Results From the Phase III Randomized ADAURA Trial. Journal of Clinical Oncology. 2023;41(10):1830-1840.
206. Belluomini L, Riva ST, Simbolo M, et al. Anticipating EGFR Targeting in Early Stages of Lung Cancer: Leave No Stone Unturned. Cells. 2021 Oct 7;10(10).
207. Belluomini L, Dodi A, Caldart A, et al. A narrative review on tumor microenvironment in oligometastatic and oligoprogressive non-small cell lung cancer: a lot remains to be done. Transl Lung Cancer Res. 2021 Jul;10(7):3369-3384.

7. APPENDIX

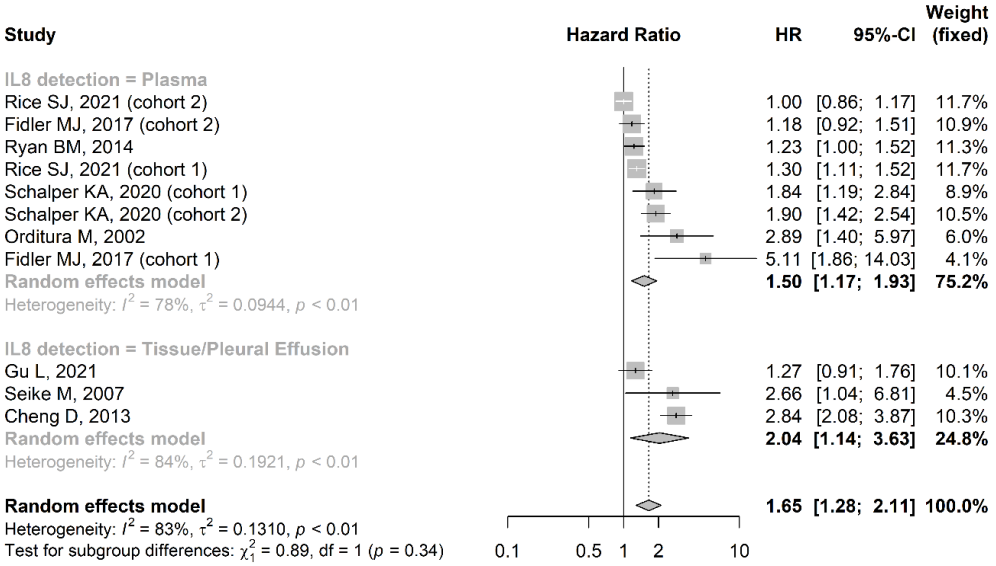

Figure A1. Forest plot of hazard ratios (HR) comparing OS in normal IL8 and overexpressed IL8 patients divided by IL8 detection. HRs for each trial are represented by the squares, and the horizontal line crossing the squares represents the 95% confidence interval (CI). The diamonds represent the estimated overall effect based on the meta-analysis random effects of the trials. All statistical tests were two sides. The plot shows no significant difference between the two subgroups but a significant effect in each subgroup.

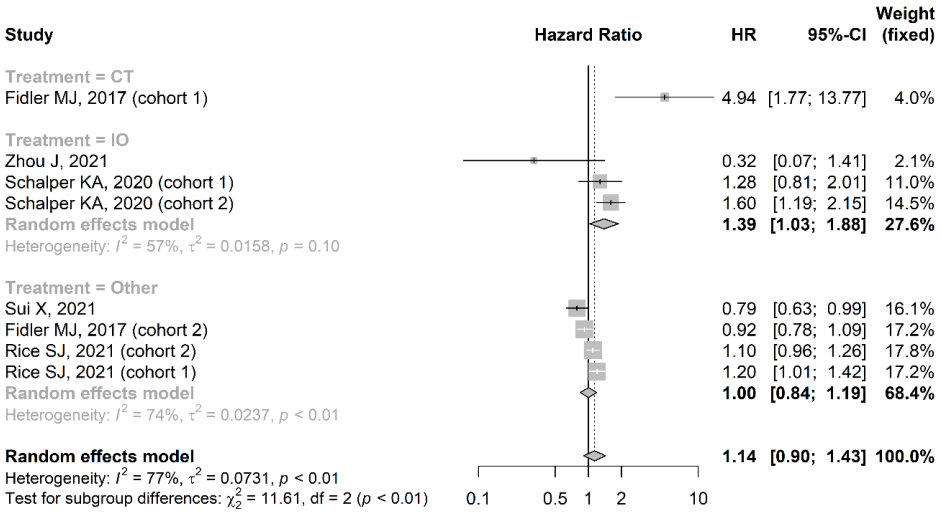

Figure A2. Forest plot of hazard ratios (HR) comparing PFS in normal IL8 and overexpressed IL8 patients divided by therapy. HRs for each trial are represented by the

squares, and the horizontal line crossing the squares represents the 95% confidence interval (CI). The diamonds represent the estimated overall effect based on the meta-analysis random effects of the trials. All statistical tests were two sides. The plot shows significant difference between the three subgroups but no significant effect for the other treatment subgroups.

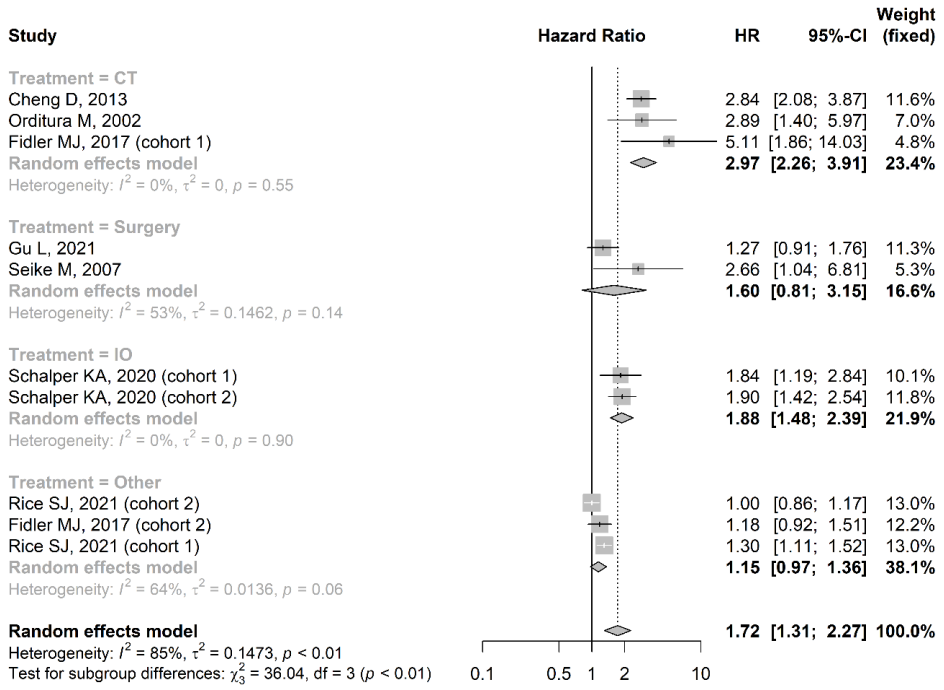

Figure A3. Forest plot of hazard ratios (HR) comparing OS in normal IL8 and overexpressed IL8 patients divided by therapy. HRs for each trial are represented by the squares, and the horizontal line crossing the squares represents the 95% confidence interval (CI). The diamonds represent the estimated overall effect based on the meta-analysis random effects of the trials. All statistical tests were two sides. The plot shows a significant difference for CT and IO subgroups and a significant difference between subgroups.

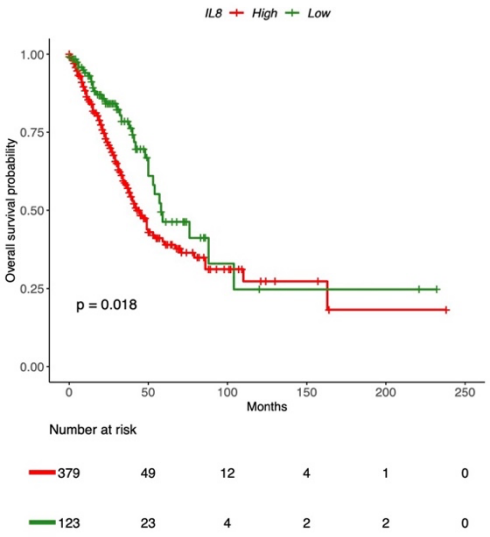

Figure A4. Kaplan-Meier curves showing the overall survival probability of LUAD patients of the TCGA dataset stratified for IL8 high and low expression (see methods section).

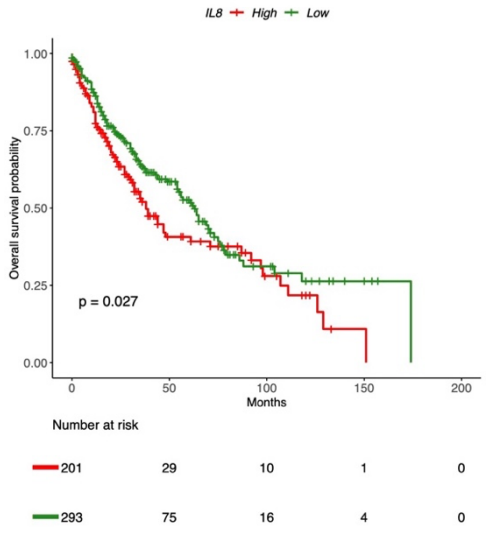

Figure A5. Kaplan-Meier curves showing the overall survival probability of LUSC patients of the TCGA dataset stratified for IL8 high and low expression (see methods section).